Journal of Medicinal Chemistry Article

J. Med. Chem. **2010,** *53,* 8319–8329 **8319**
DOI: 10.1021/jm100838z

Identification of the Spiro(oxindole-3,3′-thiazolidine)-Based Derivatives as Potential p53 Activity Modulators

Isabel Gomez-Monterrey,[†] Alessia Bertamino,[†] Amalia Porta,[‡] Alfonso Carotenuto,[†] Simona Musella,[‡] Claudio Aquino,[†] Ilaria Granata,[‡] Marina Sala,[‡] Diego Brancaccio,[†] Delia Picone,[§] Carmine Ercole,[§] Paola Stiuso,[∥] Pietro Campiglia,[‡] Paolo Grieco,[†] Pio Ianelli,[‡] Bruno Maresca,[‡] and Ettore Novellino*[,†]

[†]*Department of Pharmaceutical and Toxicological Chemistry, University of Naples "Federico II", Italy,* [‡]*Department of Pharmaceutical Science, Division of BioMedicine, University of Salerno, Italy,* [§]*Department of Chemistry, University of Naples "Federico II", Italy, and* [∥]*Department of Biochemistry and Biophysics, Second University of Naples, Naples, Italy*

Received July 6, 2010

Here, we report the design of new analogues of spirooxoindolepyrrolidine nucleus as modulators of p53 activity. Compounds (3*R*,7a*R*)-6-(4-chlorobenzyl)-1*H*-spiro[imidazo[1,5-*c*]thiazole-3,3′-indoline]-2′,5,7(6*H*,7a*H*)-trione (**9c**) and (3*R*,7a*R*)-5′-methyl-6-(3,4,5-trimethoxybenzyl)-1*H*-spiro[imidazo-[1,5-*c*]thiazole-3,3′-indoline]-2′,5,7(6*H*,7a*H*)-trione (**10d**) are the most potent compounds of this series, inhibiting cell growth of different human tumor cells at submicromolar and micromolar concentrations, respectively. Compound **9c** induces apoptotic cell death in human melanoma cell line M14 at 24 h, while in the same condition, treatment with **10d** showes a clear arrest at G2/M phase inducing delay of cell cycle progression. Possibly, these activities may be due to inhibition of p53−MDM2 interaction and subsequent p53 release and activation.

Introduction

The ability of p53 to respond to stress signals by triggering cell-cycle arrest and cell death by apoptosis is crucial to inhibit tumor development and for the response to anticancer therapy.[1−3] Inactivation of p53 by mutation occurs in about half of all human tumors.[4] Tumors that retain wild-type p53 often acquire an alternative mechanism for its inactivation, largely through deregulation of MDM2 (murin double minute-2) protein. Negative regulation of p53 activity and stability is enhanced in many human tumors and effectively impairs the activities of the p53 pathway.[5−8] Therefore, recovery of p53 activity in cancer cells by antagonizing MDM2 has been proposed as a novel approach for treating cancer and validated in vitro by macromolecular studies.[9−11] More recently, genetic and biochemical analysis of the p53−MDM2 interaction have revealed structural features suggesting that it might be targetable by small molecules.[12]

The interaction of MDM2 and p53 was shown to be mediated by a deep well-defined hydrophobic cavity on the surface of MDM2.[13] This cleft is filled only by three side chains of the helical region of p53, making this site an attractive target to design a small molecule able to mimic the contacts and the orientations of these key amino acids, thereby disrupting p53−MDM2 interaction.[14] Several low molecular weight inhibitors, including [2.2.1]bicyclic derivatives[15] sulfonamides[16] and benzodiazepinediones[17] have been identified and reported (Figure 1). The first potent and selective small molecule identified as an antagonist of the p53−MDM2 interaction, both in vitro and in vivo, were the *cis*-imidazolidines nutlins. These molecules inhibit xenograft tumor growth with no reported side effects in normal murine tissues.[18] More recently, Wang et al. used structure-based design to develop a new class of small molecule p53−MDM2 antagonists based on a spiro-oxindole core.[19] All these inhibitors share a common design of a rigid heterocyclic scaffold that can be functionalized with the appropriate side chains. A different type of inhibitor of the p53−MDM2 interactions, termed RITA,[20] activates p53 by a nongenotoxic mechanism involving the disruption of this interaction. However, RITA binds to p53 and not to MDM2. The mechanism by which it interferes with p53−MDM2 binding and its effects on the functionality of p53 are not fully understood yet.

On the basis of these findings and on identification of new activators of p53 pathway in tumor cells, we have designed and synthesized two focused libraries of compounds based on the spiro(oxindole-3,3′-thiazolidine) nucleus, a structural analogue of spirooxoindole pyrrolidine template.[21] Recently, we have described the use of this template to construct new heterocyclic systems designed as potential modulators of cell cycle.[22] In this context, the 3′,4′ hydantoin derived tetracyclic nucleus has turned out to be a very easily derivatizable scaffold. In particular, N-6 and N-1′ positions were substituted with aryl and alkyl groups (Figure 2).

In our design strategy, oxoindole, aryl, and alkyl groups are supposed to mimic the critical p53 residues that binds MDM2, i.e., Trp23, Phe19, and Leu26, respectively, while the imidazo-[1,5-*c*]thiazole nucleus would define the orientation among them. For the construction of the first library, we selected derivatives containing weak releasing (CH_3) and acceptor (Br) electron groups on the oxoindole moiety and benzyl substituted or 4,4-dimethylcyclohexyl side chain on the imidazo-thiazoledione scaffold. On the basis of the "three finger pharmacophore model" described by Dömling[23] and according

*To whom correspondence should be addressed. Phone: +39-081-678643. Fax: +39-081-678644. E-mail: novellin@unina.it.

Published on Web 11/08/2010

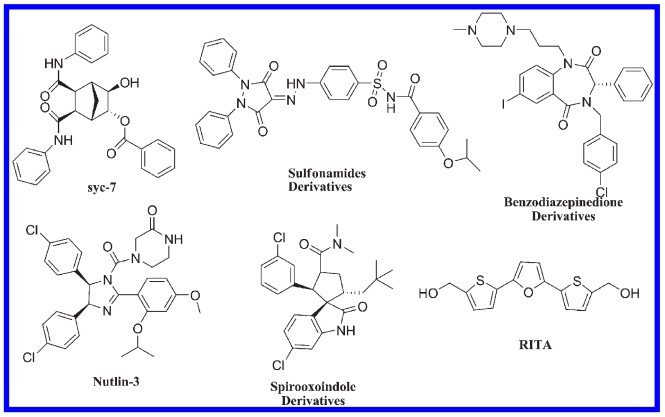

Figure 1. Small-molecule inhibitors of p53−MDM2 interaction.

to the preliminary results of cytotoxic activities, we further developed, from the most interesting compounds, a series of derivatives containing a third hydrophobic group. In this case, benzoyl, 4-methylbenzoyl, 4-chlorobenzoyl, and propyonyl groups were introduced into our template at the N-1 position (Figure 2).

The aims of the current study were to screen a range of appropriately functionalized spiro[imidazo[1,5-*c*]thiazole-3,3′-indoline]-2′,5,7(6*H*,7a*H*)-trione derivatives for cytotoxicity against different cancer cell lines and to explore some of the basic biochemical events correlated to their activity using a range of cell based approaches. The present manuscript deals with the synthesis of this new series of derivatives and with the understanding of their cytotoxic activity, the mechanism of cell cycle perturbation, the p53 expression, and the inhibition of p53−MDM2 interaction.

Results and Discussion

Chemistry. The new 5′,6-disubstituted spiro[imidazo-[1,5-*c*]-thiazole-3,3′-indoline]-2′,5,7(6*H*,7a*H*)-trione derivatives (**9a**−**e**/**12a**−**e**, Table 1) were prepared applying the synthetic route shown in Scheme 1. The starting spiro-(oxoindolethiazolidine) ethyl ester derivatives (**5**−**8**) were obtained with 80−90% yields through microwave assisted condensation between the corresponding isatin derivatives (**1**−**4**) and cysteine ethyl ester as we described previously.[22] The reaction with triphosgene in tetrahydrofuran and triethylamine followed by the in situ addition of amines (**a**−**e**) led to the corresponding *N*-carbamoyl derivatives, **9′**−**12′**, as a single isomer as observed by NMR spectrum. The synthesis of 3′-*N*-carbamoyl intermediates starting from spiro(oxoindolethiazolidine) ethyl ester derivatives **5**−**7** (R_1 = H) was strongly influenced by the solvent. Thus, the use of CH_2Cl_2 gave exclusively 1-*N*-carbamoyl derivatives while the reaction performed in THF[a] led to the formation of the desired 3′-N intermediate.

The intramolecular cyclization of these derivatives was performed in methanol in the presence of TEA at reflux

[a] Abbreviations: THF, tetrahydrofuran; TEA, triethylamine; NOE, nuclear Overhauser effect; DMSO, dimethylsulfoxide; HSQC, heteronuclear single-quantum coherence spectra; AIDA, antagonist induced dissociation assay; TLC, thin-layer chromatography; MS, mass spectrometry; ESI, electrospray ionization; PBS, phosphate buffered saline; EDTA, ethylenediaminetetraacetic acid; TBS, Tris buffered saline; IPTG, isopropyl β-D-1-thiogalactopyranoside; OD_{600nm}, optical density at 600 nm; DTT, dithiothrietol. Abbreviations used for amino acids follow the rules of the IUPAC-IUB Commission of Biochemical Nomenclature in *J. Biol. Chem.* **1972**, *247*, 977−983.

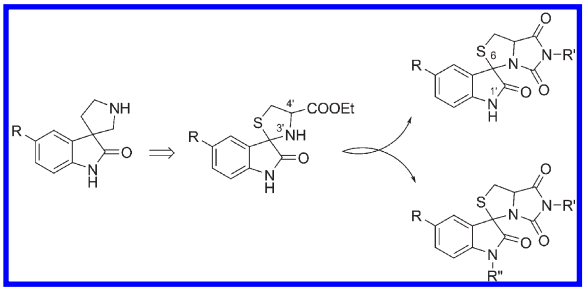

Figure 2. Design of new derivatives from spiro(oxindole-3,3′-thiazolidine): R = H, CH_3, Br; R′ = benzyl derivatives or alkyl; R″ = H or acyl derivatives.

temperature, and the corresponding spiro[imidazo[1,5-*c*]-thiazole-3,3′-indoline]-2′,5,7(6*H*,7a*H*)-trione derivatives (**9a**−**d**/**12a**−**d**) were obtained with 39−56% overall yields as simple isomer. This cyclization was stereospecific[24] toward the 3*R*,7a*R* isomer, as the corresponding C-3 epimer was not detected in the reaction mixture. The assignment of the relative configuration at the C-3 asymmetric center as 3*R* was determined on the basis of a NOE enhancement between H-4′ and H-7a observed in the 2D NOESY spectra of all compounds. Absolute configurations were defined hypothesizing configuration retention at C-7a.

Finally, the 1′-acylspiro[imidazo[1,5-*c*]thiazole-3,3′-indoline]-2′,5,7(6*H*,7a*H*)-trione derivatives (**13f**−**i**/**14f**−**i**) were prepared in 85−89% yields by treatment of starting derivatives **9c** and **10d** with the corresponding acyl chloride (**f**−**i**) as depicted in Scheme 2.

In Vitro Cytotoxicity. The spiroimidazothiazoloxoindole derivatives were examined for antiproliferative activity against three cell lines: the transformed human embryonic kidney HEK, the human melanoma M14, and the human leukemia monocyte lymphoma U937 cell lines. The obtained IC_{50} values are summarized in Table 1. Doxorubicin was used as reference cytotoxic agent. The most interesting results were obtained with the isatin **9** series. Compound **9c** containing a 4-chlorobenzyl substituent at position N-6 showed an elevated cytotoxic activity with IC_{50} values of 0.44, 0.53, and 0.87 μM in HEK, M14, and U937 cell lines, respectively. Compounds **9a**, **9b**, and **9d**, with a diverse substituted benzyl group at the N-6 position, retained the cytotoxic activity at micromolar concentration on the HEK and U930 cell lines, while they were less active in the M14 melanoma cell line. The introduction of an electron-releasing group as the $-CH_3$ group at C-5′ position of the indol ring produced different effects: while the derivative **10c** reduced activity in the three cell lines compared to **9c** (8-, 12-, and 3-fold, respectively), compounds **10a**, **10b**, and **10d** increased their biological effect in all cell lines compared to **9a**, **9b**, and **9d**. In particular, these compounds were 2- to 4-fold more potent than the corresponding analogues **9** against M14 cell line. The introduction at the C-5′ position of the isatin moiety of an electron-withdrawing group such as the bromide group caused a reduction of the activity of the corresponding analogues **11a**, **11b**, **11c**, and **11d** in all cell lines. On the other hand, substitution of an aryl group for an alkyl group at the N-6 position was tolerated only in the isatin series **9** (compound **9e**) even with a loss in activity with respect to **9c** (8-, 14-, and 4-fold in the three cell lines, respectively). Compounds **10e**, **11e**, and **12e** showed a dramatic loss of activity. Finally, the derivatives **12a**, **12c**, and **12d**, which incorporate at position N-1′ a methyl group, retained cytotoxic

Table 1. Cytotoxic Activity of Spiro[imidazo[1,5-*c*]thiazole-3,3′-indoline]-2′,5,7(6*H*,7a*H*)-trione Derivatives **9a**−**e**/**12a**−**e**

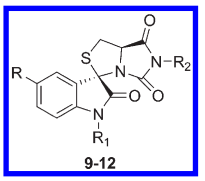

				$IC_{50} \pm SD^a$ (μM)		
compd	R	R_1	R_2	HEK[b]	M14[c]	U937[d]
9a	H	H	-$CH_2C_6H_5$	4.80 ± 0.15	10.64 ± 0.04	3.90 ± 0.01
9b	H	H	-$CH_2C_6H_4$(4-CH_3)	4.53 ± 0.15	13.27 ± 0.03	5.91 ± 0.02
9c	H	H	-$CH_2C_6H_4$(4-Cl)	0.44 ± 0.01	0.53 ± 0.01	0.87 ± 0.01
9d	H	H	-$CH_2C_6H_2$(3,4,5-OCH_3)	3.80 ± 0.08	4.73 ± 0.02	2.51 ± 0.05
9e	H	H	4-dimethylcyclohexyl	4.22 ± 0.07	7.07 ± 0.01	2.61 ± 0.05
10a	CH_3	H	-$CH_2C_6H_5$	3.30 ± 0.07	3.88 ± 0.02	2.09 ± 0.04
10b	CH_3	H	-$CH_2C_6H_4$(4-CH_3)	3.01 ± 0.06	3.39 ± 0.03	2.77 ± 0.02
10c	CH_3	H	-$CH_2C_6H_4$(4-Cl)	3.88 ± 0.05	6.65 ± 0.02	3.31 ± 0.04
10d	CH_3	H	-$CH_2C_6H_2$(3,4,5-OCH_3)	2.04 ± 0.03	2.40 ± 0.02	2.06 ± 0.04
10e	CH_3	H	4-dimethylcyclohexyl	16.01 ± 0.05	19.12 ± 0.07	12.48 ± 0.05
11a	Br	H	-$CH_2C_6H_5$	8.48 ± 0.09	12.04 ± 0.03	7.58 ± 0.05
11b	Br	H	-$CH_2C_6H_4$(4-CH_3)	7.61 ± 0.10	10.24 ± 0.10	6.23 ± 0.14
11c	Br	H	-$CH_2C_6H_4$(4-Cl)	7.13 ± 0.06	7.06 ± 0.05	5.01 ± 0.03
11d	Br	H	-$CH_2C_6H_2$(3,4,5-OCH_3)	9.31 ± 0.09	11.04 ± 0.02	5.02 ± 0.03
11e	Br	H	4-dimethylcyclohexyl	> 40	> 40	> 40
12a	H	CH_3	-$CH_2C_6H_5$	3.98 ± 0.05	6.37 ± 0.04	2.89 ± 0.03
12b	H	CH_3	-$CH_2C_6H_4$(4-CH_3)	10.71 ± 0.10	31.79 ± 0.04	16.75 ± 0.02
12c	H	CH_3	-$CH_2C_6H_4$(4-Cl)	2.11 ± 0.05	2.47 ± 0.02	2.91 ± 0.01
12d	H	CH_3	-$CH_2C_6H_2$(3,4,5-OCH_3)	6.01 ± 0.06	7.66 ± 0.23	5.70 ± 0.05
12e	H	CH_3	4-dimethylcyclohexyl	> 40	> 40	> 40
doxorubicin				0.9 ± 0.08	1.0 ± 0.05	0.8 ± 0.01

[a] Data represent mean values (SD) of three independent determinations. [b] Transformed human embryonic kidney cell line. [c] Human melenoma cell line. [d] Human leukemia monocyte lymphoma.

Scheme 1. Synthesis of Spiro[imidazo[1,5-*c*]-thiazole-3,3′-indoline]-2′,5,7(6*H*,7a*H*)-trione Derivatives **9a**−**e**/**12a**−**e**[a]

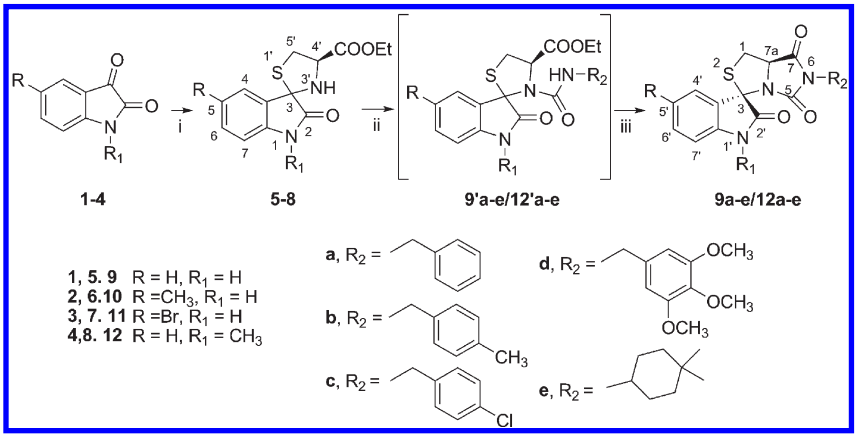

[a] Reagents and conditions: (i) Cys-OEt, $NaHCO_3$ in MeOH, microwave; (ii) triphosgene, TEA, THF, room temp, 10 min, then R_2-NH_2; (iii) MeOH, TEA, reflux, 1−3 h.

levels within the micromolar range. The same substitution was detrimental for the activity of analogues **12b** and **12e**.

The preliminary results on citotoxicity and morphological cellular differences after treatment with **9c** and **10d** (see below) motivated us to study further the mode of action of these compounds. We have performed a comparative analysis of their effects on growth in immortalized normal thyroid TAD-2 and human papillary thyroid carcinoma TPC1 cell lines to establish a safety profile of these derivatives. Inhibition of proliferation of both cell lines was measured after treatment with 100 nM and 1 μM of **9c** and **10d** at 48 h.

Figure 3a shows that at 100 nM, **9c** and **10d** caused a net decrease in the total number of cells in the carcinoma TPC1 cell line (70% and 58%, respectively), whereas the percentage of cellular growth inhibition in the TAD-2 cell line was only of 10% for **9c** and void for **10d** (Figure 3b). At 1 μM, both compounds were cytotoxic for the TAD-2 cell line. These data seem to indicate that at 100 nM, **9c** and **10d** have a good profile of "cell selectivity".

Futhermore, the introduction into **9c** and/or **10d** of a third hydrophobic group at the N-1′ position appeared to have an important effect upon cytotoxicity, particularly in the case of

Scheme 2. Synthesis of 1′-Acylspiro[imidazo[1,5-*c*]thiazole-3,3′-indoline]-2′,5,7(6*H*,7a*H*)-trione derivatives (**13f−i**/**14f−i**)

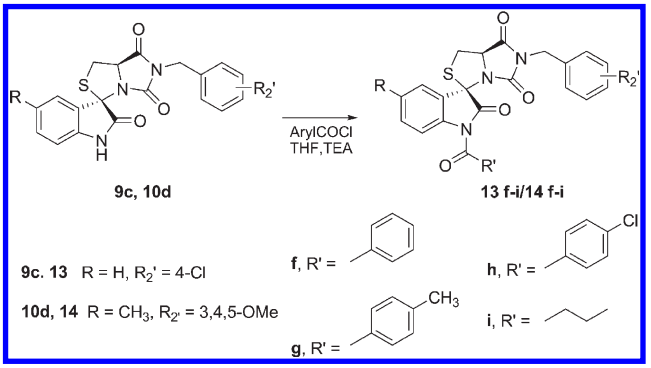

compounds **13**. Derivatives **13f−i** were 3- to 10-fold less potent than the corresponding analogue **9c**, though they maintain their activity in the micromolar range (IC_{50} of 2.01−5.01 μM, Table 2). These results are in agreement with those found for **12c** (IC_{50} of 2.11−2.91 μM, Table 1), which has a CH_3 group at the N-1′ position, indicating that the introduction of hydrophobic groups in this position limits the optimal side chain accommodation in the target, independent of their electronic and steric properties.

The introduction of acyl side chains in N-1′ position of **10d** led to slight or moderate decreases in the cytotoxic activity. Derivatives **14f−i** were only 1.5- to 3-fold less active than their analogue **10d**. These findings imply a lower tolerance of compound **9c** to structural modification.

Phase-Contrast Microscopic Analysis of Cell Morphology and Apoptosis. Figure 4 shows that vehicle-treated M14 cells grew normally, while treatment with **9c** and **10d** impaired their morphology as determined by video time lapse microscopy. A 10 h treatment with these compounds caused the emergence of round and damaged shapes followed by the formation of numerous blebs and a progressive detachment from the plastic well (48 h treatment).

Treated cells displayed a lower number of cell division compared to control cells (Figure 4). These modifications were more pronounced and appeared earlier in cell cultures treated with **9c** than with **10d** and were consistent with induction of apoptotic cell death.[25] To confirm this observation, we measured caspase-3 activity. Upon cleavage by upstream proteases in an intracellular cascade, the activation of caspase-3 is considered a hallmark of the apoptotic process.[26] The levels of cleaved active subunits of executioner caspase-3 were evaluated by Western blotting of M14 cell lysates following **9c** (0.1−0.3 μM) and **10d** (1.0−5.0 μM) treatment for 16 and 24 h (Figure 5a). Compound **10d** did not lead to any caspase cleavage even at supra-IC_{50} concentration. **9c** increased caspase-3 activity after a 16 h exposure. Next, we examined the activation-mediated cleavage of caspase-3 substrate, poly(ADP-ribose) polymerase (PARP), which is a reliable marker of apoptosis (Figure 5b).[27] By use of the cysteine protease activity, caspases separate N-terminal DNA-binding domain of PARP from its C-terminal catalytic domain (85 kDa) showing that **9c** increased caspase-3 activity and PARP cleavage following 16 h of exposure, suggesting that **9c** induced apoptotic cell death in M14 cells. On the contrary, after 24 h and at cytotoxic concentration, compound **10d** did not induce apoptotic death

Cell Cycle Effects and Expression of p53. On the basis of previous data, we analyzed the effect of **9c** and **10d** on cell

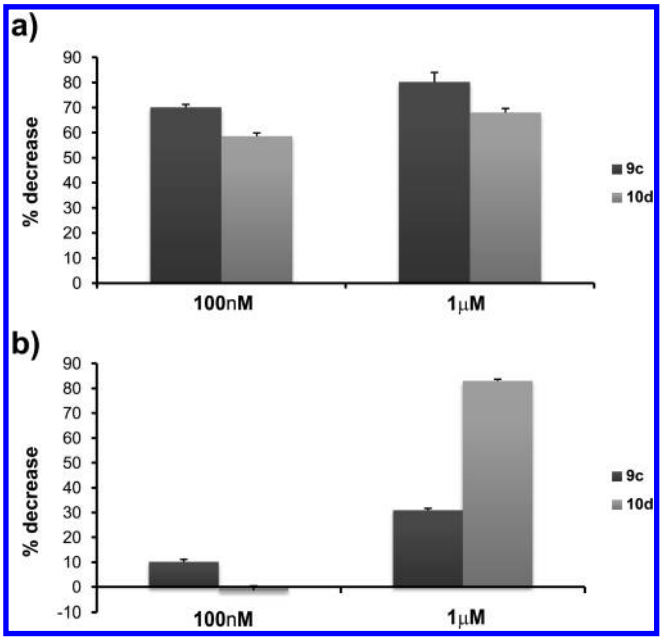

Figure 3. Effect of **9c** and **10d** derivatives on cell growth of (a) human papillary thyroid carcinoma TPC1 and (b) normal thyroid TAD-2 cell lines.

cycle progression. The cytometric investigation showed a clear arrest at G2/M cell cycle phase of M14 cells treated with **10d** (3 μM) for 24 h compared to control cells (Figure 6a). Accumulation of cells in the G2 phase increased about 47% ($p < 0.001$) with a corresponding decrease of cells in the G0/G1 phase (down to 20%, $p < 0.001$). Under the same conditions, treatment of M14 cells with **9c** (0.3 and 1 μM) did not show any significant effect on the cell cycle progression. The arrest of cell cycle induced by **10d** correlated well with a decreased expression of cyclin B1 compared to the control cells (Figure 6b), indicating that cell cycle progression of cells in the G2/M phase was markedly delayed and cells did not progress into M phase.

Subsequently, we examined expression of the p53 as key regulator of both cell-cycle arrest and cell apoptotic death. Treatment of M14 cells with subcytotoxic concentrations of **9c** and **10c** produced, in both cases, a gradual increase of the p53 levels from 24 to 48 h. As observed in Figure 7, this increase is more significant in the case of **9c** at 24 h compared to control cells.

Inhibition of p53−MDM2 Interaction. The ability of compounds **9c** and **10d** to block p53−MDM2 interaction was investigated by NMR analysis. Holak et al. have recently described a two-dimensional ^{15}N-HSQC based NMR assay to determine the effect of antagonists on protein−protein interactions.[28] The method, named AIDA (for antagonist induced dissociation assay), provides information on whether an antagonist of a protein−protein interaction is strong enough to dissociate the complex and whether its mode of action is modulated by denaturation, precipitation, or release of a protein in its functional folded state. AIDA requires the use of a large protein fragment (larger than 30 kDa) to bind to a small reporter protein (less than 20 kDa). In appropriate conditions (flexible residues), 1D proton NMR spectra may suffice for monitoring the states of proteins in complexes upon treatment with ligands. Because of the highly flexible nature of the N-terminal domain of p53, p53−MDM2 complex is suitable for 1D proton NMR application.

Table 2. Cytotoxic Activity of 1′-Acylspiro[(dihydroimidazo[1,5-*c*]-thiazolo-5,7-dione)-3,3′-(dehydroindol-2-one)] Derivatives **13f−i**/**14f−i**

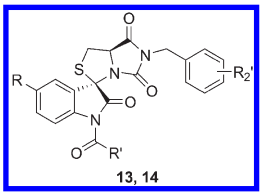

compd	R	R_1'	R_2'	$IC_{50} \pm SD^a$ (μM) HEK	M14	U937
9c	H		4-Cl	0.44 ± 0.01	0.53 ± 0.01	0.87 ± 0.01
13f	H	-C_6H_5	4-Cl	3.50 ± 0.02	3.25 ± 0.36	3.12 ± 0.07
13g	H	-C_6H_4(4-CH_3)	4-Cl	2.50 ± 0.10	2.08 ± 0.10	2.01 ± 0.15
13h	H	-C_6H_4(4-Cl)	4-Cl	5.01 ± 0.15	3.37 ± 0.37	2.61 ± 0.05
13i	H	-$CH_2CH_2CH_3$	4-Cl	2.01 ± 0.05	2.04 ± 0.34	2.10 ± 0.09
10d	CH_3		3,4,5-OCH_3	2.04 ± 0.03	2.40 ± 0.02	2.06 ± 0.04
14f	CH_3	-C_6H_5	3,4,5-OMe	4.22 ± 0.14	7.84 ± 0.02	4.31 ± 0.02
14g	CH_3	-C_6H_4(4-CH_3)	3,4,5-OMe	3.81 ± 0.05	5.95 ± 0.01	2.42 ± 0.04
14h	CH_3	-C_6H_4(4-Cl)	3,4,5-OMe	4.71 ± 0.15	8.14 ± 0.02	3.11 ± 0.01
14i	CH_3	-$CH_2CH_2CH_3$	3,4,5-OMe	4.42 ± 0.16	7.40 ± 0.0126	4.10 ± 0.02

[a] Data represent mean values (SD) of three independent determinations.

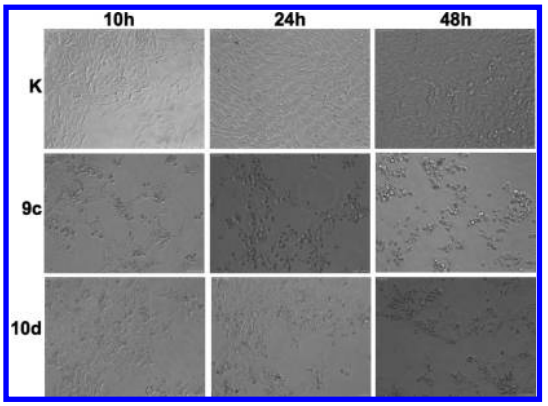

Figure 4. Morphological changes induced by treatment of M14 cell line with **9c** and **10d** after 10, 24, and 48 h at IC_{50} concentration. Cells had a doubling time of 19 h in culture (confirmed by cell counts, data not shown).

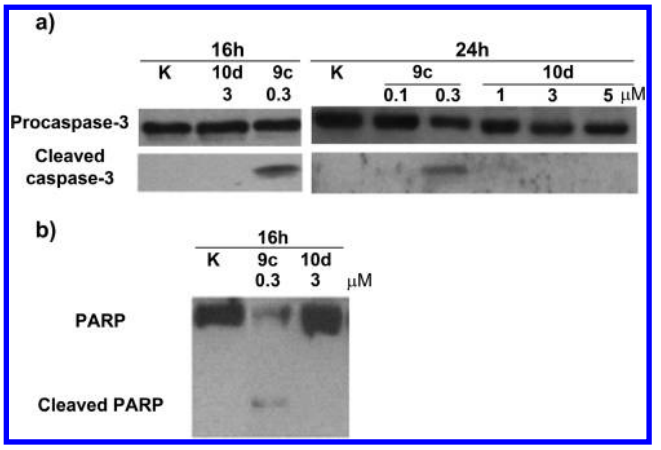

Figure 5. Caspase-3 (a) and PARP (b) cleavages induced for **9c** and **10d**.

In particular, the $^{N}H^{\varepsilon}$ side chains of W23 and W53 produce sharp lines in the free p53 1D proton spectrum. On formation of the complex with MDM2, W23 signal disappears, since W23, together with the p53 residues 17−26, comprises the primary binding site for MDM2. Upon binding, these residues participate in well-defined structures of large p53−MDM2 complexes, whereas W53 is still not structured when p53 is bound to MDM2.[28,29] The observed $1/T_2$ transverse relaxation rate of the bound W23 in the complexes increases significantly, and the broadening of NMR resonances results in the disappearance of this signal from the spectra. Figure 8a shows the NMR spectrum of the tryptophan residues of the p53−MDM2 complex (only W53 $^{N}H^{\varepsilon}$ side chains signal can be detected). After the addition of **9c** or **10d** to the p53−MDM2 complex, the W23 peak appears (Figure 8b and Figure 8c, respectively). Nutlin-3 was also used as positive control (Figure 8d), causing a complete p53 release.[28] Both compounds **9c** and **10d** released p53−MDM2 complex but were not as efficient as nutlin-3 causing about 80% and 60% p53 release, respectively.

Conclusion

Here we report the design, synthesis, and biological evaluation of new spiro[imidazo[1,5-*c*]thiazole-3,3′-indoline]-2′,5,7-trione derivatives which exhibit activity against different tumor cell lines. In particular, compound **9c** showed high efficacy in HEK-293 (kidney), M-14 (melanoma), and U937 (leukemia) human cell lines with IC_{50} values of 0.44, 0.53, and 0.87 μM, respectively. The derivative containing a trimetoxybenzyl group at N-6 position, **10d**, was 3- to 5-fold less cytotoxic in all tested cell lines and showed a time-dependent activity different from that of **9c**. Preliminary studies on the induction of apoptosis and cell cycle progression in M14 cell line confirmed a different behavior of these compounds. Compound **9c** induced apoptotic cell death after 24 h of treatment at cytotoxic concentration, while **10d** did not induce apoptotic death in the same period of time. On the other hand, **10d** markedly prolonged the G2 phase, causing a delay of cell cycle progression in responsive cells, while treatment with **9c** did not alter the normal course of cell cycle. However, both compounds induce a time-dependent increment of p53 expression, indicating that the activity profiles of these

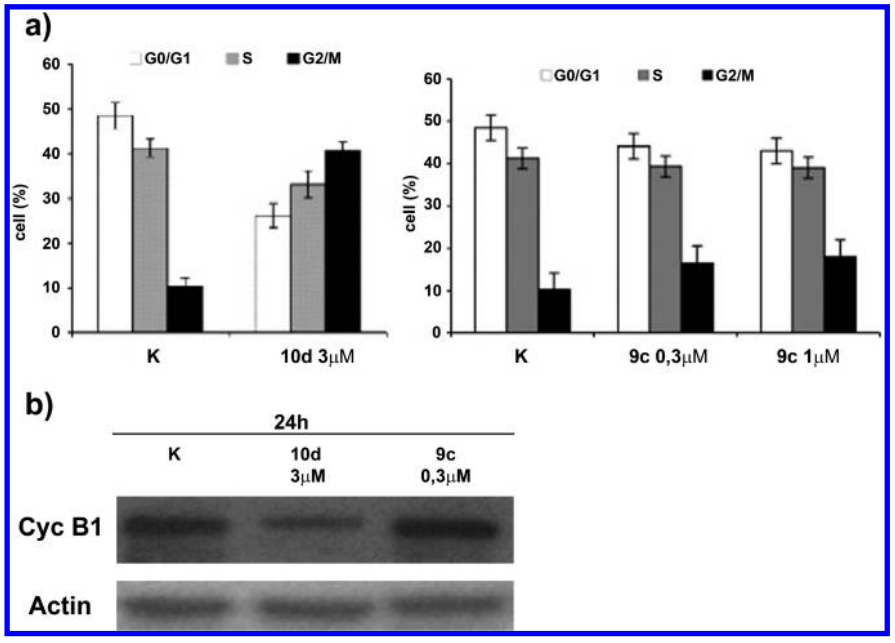

Figure 6. Effects of **9c** and **10d** on the distribution of cell populations. Data represent the percentage of cells in each cellular cycle phase (a). Shown is the Western blot expression of cyclin B1 in the control and induced by **9c** and **10d** (b).

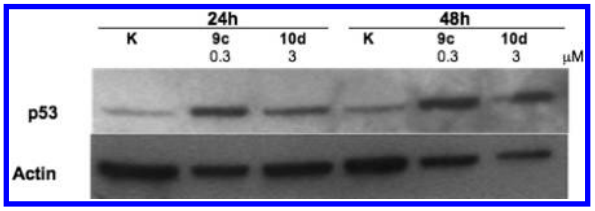

Figure 7. Western blot analysis of cytoplasmatic p53 levels in M14 cells untreated (K) and treated with **9c** (0.3 μM) and **10d** (3 μM) after 24 and 48 h.

derivatives might be regulated by this protein. NMR investigation performed on compounds **9c** and **10d** demonstrated that the ability of these compounds to block p53−MDM2 interaction caused release of p53. Taken together, these findings show that chemical modification at the pyrrolidine moiety of spirooxoindole system is an effective approach to study the modulation of p53 activity through p53−MDM2 inhibition. Further experiments aimed both to identify more potent and selective spirothiazolidin-based derivatives and to better understand the mechanisms of inhibition of growth are currently underway.

Experimental Section

General. Reagents, starting materials, and solvents were purchased from commercial suppliers and used as received. Analytical TLC was performed on plates coated with a 0.25 mm layer of silica gel 60 F254 Merck and preparative TLC on 20 cm × 20 cm glass plates coated with a 0.5 mm layer of silica gel PF254 Merck. Silica gel 60 (300−400 mesh, Merck) was used for flash chromatography. Melting points were determined by a Kofler apparatus and are uncorrected. Optical rotations were measured on an Atago Polax 2-L polarimeter. ^{1}H NMR and ^{13}C NMR spectra were recorded with a Varian-400 spectrometer, operating at 400 and 100 MHz, respectively. Chemical shifts are reported in δ values (ppm) relative to internal Me_4Si, and J values are reported in hertz (Hz). ESIMS experiments were performed on an Applied Biosystem API 2000 triple-quadrupole spectrometer. Starting spiro(oxoindolethiazolidine) ethyl ester derivatives (**5**−**8**) were synthesized as described in ref 22. Combustion

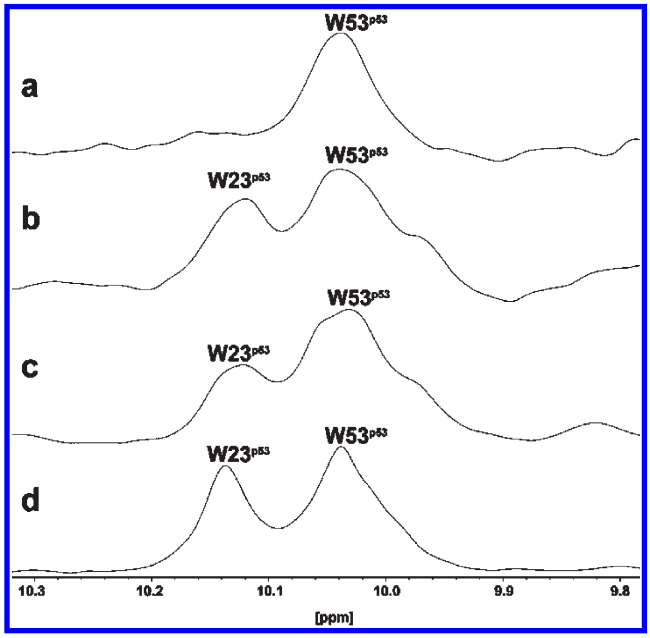

Figure 8. One-dimensional proton spectrum of the side chains of tryptophans (W) of p53−MDM2 complex (a) and after addition of **9c** (b), **10d** (c), and nutlin-3 (d).

microanalyses were performed on a Carlo Erba CNH 1106 analyzer, and all reported values are within 0.4% of calculated values. These elemental analyses confirmed >95% purity.

General Procedure for the Synthesis of the (3*R*,7a*R*)-6-(Alkyl or benzylsubstituted)-spiro[imidazo[1,5-*c*]thiazole-3,3′-indoline]-2′,5,7(6*H*,7a*H*)-trione Derivatives (9a−e/12a−e). Triphosgene (0.3 mmol) and TEA (0.9 mmol) were added to a solution of (2′*R*,4′*R*)- and (2′*S*,4′*R*)-ethyl 2-oxospiro[indoline-3,2′-thiazolidine]-4′-carboxylate derivatives (**5**−**8**, 200 mg, 0.7 mmol) in dry THF (15 mL). After the mixture was stirred at room temperature for 10 min, a solution in dry THF of corresponding amines (benzylamine, 4-methylbenzylamine, 4-chlorobenzylamine, 3,4,5-trimethoxybenzylamine, or 4,4-dimethylcicloesilamine, **a**−**e**) (0.75 mmol) was added. The reaction mixture was then

stirred at room temperature for 3 h. Solvent was evaporated, and the residue was dissolved in dichloromethane. The organic solution was washed with water (3 × 100 mL), dried over Na_2SO_4, and evaporated in vacuo. The residues were dissolved in MeOH and TEA until pH 8.0 was obtained, and the mixture was heated to reflux temperature for 2 h. The mixture was then cooled to ambient temperature, and solvent was removed in vacuo. The residue was dissolved in dichloromethane and washed with water (3 × 100 mL). Flash chromatography on silica gel, using ethyl acetate/*n*-hexane in 3/2 ratio as eluent, yielded the correspondent final derivatives. The achieved compounds were crystallized with MeOH to give white solids.

(3*R*,7a*R*)-6-Benzyl-1*H*-spiro[imidazo[1,5-*c*]thiazole-3,3′-indoline]-2′,5,7(6*H*,7a*H*)-trione (9a). Yield 44%, mp 181−182 °C, $[\alpha]^{25}_D$ −6.9° (*c* 0.11, MeOH). ^{1}H NMR (400 MHz, $CDCl_3$) δ 3.35 (dd, 1H, *J* = 5.6 and 11.6 Hz, Ha-1); 3.72 (t, 1H, Hb-1); 4.56 (d, 1H, *J* = 14.8 Hz, CH_2); 4.71 (d, 1H, CH_2); 5.00 (dd, 1H, *J* = 5.6 and 11.2 Hz, H-7a); 6.83 (d, 1H, *J* = 7.6 Hz, H-7′); 7.07 (t, 1H, H-6′); 7.26−7.34 (m, 6H, H-5′ and aryl); 7.39 (d, 1H, H-4′); 7.81 (s, 1H, N*H*). ^{13}C NMR (100 MHz, $CDCl_3$) δ 32.4 (C-1), 43.0 (*C*H_2), 68.9 (C-7a), 70.1 (C-3), 110.3, 123.4, 125.3, 125.8, 129.1, 130.2, 131.5, 133.4, 135.4, 138.2 (aryl), 156.3, 169.9, 176.0 (C═O). ESIMS *m*/*z* calcd for $C_{19}H_{15}N_3O_3S$, 365.08; found, 365.13.

(3*R*,7a*R*)-6-(4-Methylbenzyl)-1*H*-spiro[imidazo[1,5-*c*]thiazole-3,3′-indoline]-2′,5,7(6*H*,7a*H*)-trione (9b). Yield 48%, mp 212−213 °C, $[\alpha]^{25}_D$ −7.1° (*c* 0.1, MeOH). ^{1}H NMR (400 MHz, $CDCl_3$) δ 2.29 (s, 3H, CH_3); 3.33 (dd, 1H, *J* = 5.6 and 11.2 Hz, Ha-1); 3.71 (t, 1H, Hb-1); 4.51 (d, 1H, *J* = 14.4 Hz, CH_2); 4.67 (d, 1H, CH_2); 4.97 (dd, 1H, *J* = 5.6 and 10.8 Hz, H-7a); 6.81 (d, 1H, *J* = 7.6 Hz, H-7′); 7.04−7.11 (m, 6H, H-6′ and aryl); 7.28 (t, 1H, H-5′); 7.37 (d, 1H, *J* = 7.6 Hz, H-4′); 8.06 (s, 1H, N*H*). ^{13}C NMR (100 MHz, $CDCl_3$) δ 21.2 (*C*H_3), 32.5 (C-1), 43.1 (*C*H_2), 68.9 (C-7a), 70.2 (C-3), 110.9, 123.6, 125.3, 125.9, 128.1, 128.4, 128.9, 131.7, 133.4, 135.2, 138.0 (aryl), 156.4, 169.6, 176.2 (C═O). ESIMS *m*/*z* calcd for $C_{20}H_{17}N_3O_3S$, 379.10; found, 379.18.

(3*R*,7a*R*)-6-(4-Chlorobenzyl)-1*H*-spiro[imidazo[1,5-*c*]thiazole-3,3′-indoline]-2′,5,7(6*H*,7a*H*)-trione (9c). Yield 48%, mp 205−206 °C, $[\alpha]^{25}_D$ −8.8° (*c* 0.12, MeOH). ^{1}H NMR (400 MHz, $CDCl_3$) δ 3.35 (dd, 1H, *J* = 5.6 and 11.2 Hz, Ha-1); 3.71 (t, 1H, Hb-1); 4.53 (d, 1H, *J* = 15.2 Hz, CH_2); 4.67 (d, 1H, CH_2); 5.00 (dd, 1H, *J* = 5.6 and 10.8 Hz, H-7a); 6.78 (d, 1H, *J* = 8.0 Hz, H-7′); 7.06 (t, 1H, H-6′); 7.25−7.30 (m, 5H, H-5′ and aryl); 7.39 (d, 1H, H-4′); 8.43 (s, 1H, N*H*). ^{13}C NMR (100 MHz, $CDCl_3$) δ 32.4 (C-1), 42.5 (*C*H_2), 68.9 (C-7a), 70.1 (C-3), 111.2, 123.7, 125.3, 125.4, 129.2, 130.1, 131.2, 133.8, 134.2, 140.8 (aryl), 156.4, 169.9, 176.1 (C═O). ESIMS *m*/*z* calcd for $C_{19}H_{14}ClN_3O_3S$, 399.04; found, 399.13.

(3*R*,7a*R*)-6-(3,4,5-Trimethoxybenzyl)-1*H*-spiro[imidazo[1,5-*c*]-thiazole-3,3′-indoline]-2′,5,7(6*H*,7a*H*)-trione (9d). Yield 47%, mp 219−220 °C, $[\alpha]^{25}_D$ −8.2° (*c* 0.12, MeOH). ^{1}H NMR (400 MHz, $CDCl_3$) δ 3.34 (dd, 1H, *J′* = 5.6 and 11.6 Hz, Ha-1); 3.66 (t, 1H, Hb-1); 3.72 (s, 3H, OCH_3,); 3.81 (s, 6H, OCH_3,); 4.46 (d, 1H, *J* = 14.4 Hz, CH_2); 4.64 (d, 1H, CH_2); 5.00 (dd, 1H, *J* = 5.2 and 10.6 Hz, H-7a); 6.56 (s, 2H, aryl); 6.83 (d, 1H, *J* = 7.2 Hz, H-7′); 7.09 (t, 1H, H-6′); 7.25 (t, 1H, H-5′); 7.38 (d, 1H, H-4′); 8.22 (s, 1H, N*H*). ^{13}C NMR (100 MHz, $CDCl_3$) δ 32.5 (C-1), 43.3 (*C*H_2), 56.4 (O*C*H_3), 68.9 (C-7a), 70.6 (C-3), 105.4, 110.8, 125.4, 126.0, 130.9, 131.2, 133.5, 137.2, 138.4, 154.9 (aryl), 156.3, 169.4, 175.7 (C═O). ESIMS *m*/*z* calcd for $C_{22}H_{21}N_3O_6S$, 455.12; found, 455.25.

(3*R*,7a*R*)-6-(4,4-Dimethylcyclohexyl)-1*H*-spiro[imidazo[1,5-*c*]-thiazole-3,3′-indoline]-2′,5,7(6*H*,7a*H*)-trione (9e). Yield 52%, mp 180−181 °C, $[\alpha]^{25}_D$ −8.1° (*c* 0.1, MeOH). ^{1}H NMR (400 MHz, $CDCl_3$) δ 0.89 (s, 3H, CH_3); 0.93 (s, 3H, CH_3); 1.19−1.25 (m, 2H, CH_2); 1.41−1.49 (m, 4H, CH_2); 2.21−2.33 (m, 2H, CH_2); 3.32 (dd, 1H, *J* = 5.2 and 10.8 Hz, Ha-1); 3.71 (t, 1H, Hb-1); 3.78−3.82 (m, 1H, C*H*); 4.93 (dd, 1H, *J* = 5.6 and 10.8 Hz, H-7a); 6.85 (d, 1H, *J* = 7.6 Hz, H-7′); 7.08 (t, 1H, H-6′); 7.27 (t, 1H, H-5′); 7.41 (d, 1H, H-4′); 8.06 (s, 1H, N*H*). ^{13}C NMR (100 MHz, $CDCl_3$) δ 24.8 (*C*H_2); 25.4 (*C*H_2); 26.7 (*C*H_3); 29.9 (*C*H_3); 32.3 (C-1), 38.7 (*C*H), 52.8 (*C*), 68.7 (C-7a), 70.6 (C-3), 109.6, 123.6, 125.0, 125.3, 131.1, 143.6 (aryl), 156.6, 170.5, 174.6 (C═O). ESIMS *m*/*z* calcd for $C_{20}H_{23}N_3O_3S$, 385.15; found, 385.21.

(3*R*,7a*R*)-6-Benzyl-5′-methyl-1*H*-spiro[imidazo[1,5-*c*]thiazole-3,3′-indoline]-2′,5,7(6*H*,7a*H*)-trione (10a). Yield 45%, mp 193−194 °C, $[\alpha]^{25}_D$ −12.4° (*c* 0.11, MeOH). ^{1}H NMR (400 MHz, $CDCl_3$) δ 2.30 (s, 3H, CH_3); 3.33 (dd, 1H, *J* = 5.2 and 11.2 Hz, Ha-1); 3.73 (t, 1H, Hb-1); 4.56 (d, 1H, *J* = 14.8 Hz, CH_2); 4.71 (d, 1H, CH_2); 5.00 (dd, 1H, *J* = 5.6 and 10.8 Hz, H-7a); 6.70 (d, 1H, *J* = 8.0 Hz, H-7′); 7.05 (d, 1H, H-6′); 7.23 (s, 1H, H-4′); 7.26−7.36 (m, 5H, aryl); 8.11 (s, 1H, N*H*). ^{13}C NMR (100 MHz, $CDCl_3$) δ 21.2 (*C*H_3); 32.4 (C-1), 43.2 (*C*H_2), 68.9 (C-7a), 70.3 (C-3), 110.9, 125.3, 126.0, 128.3, 128.7, 128.9, 131.6, 133.4, 135.4, 138.2 (aryl), 156.4, 169.9, 176.0 (C═O). ESIMS *m*/*z* calcd for $C_{20}H_{17}N_3O_3S$, 379.10; found, 379.23.

(3*R*,7a*R*)-5′-Methyl-6-(4-methylbenzyl)-1*H*-spiro[imidazo-[1,5-*c*]thiazole-3,3′-indoline]-2′,5,7(6*H*,7a*H*)-trione (10b). Yield 45%, mp 234−235 °C, $[\alpha]^{25}_D$ −12.5° (*c* 0.11, MeOH). ^{1}H NMR (400 MHz, $CDCl_3$) δ 2.30 (s, 6H, CH_3); 3.31 (dd, 1H, *J* = 5.6 and 11.6 Hz, Ha-1); 3.71 (t, 1H, Hb-1); 4.51 (d, 1H, *J* = 14.8 Hz, CH_2); 4.67 (d, 1H, CH_2); 4.97 (dd, 1H, *J* = 5.2 and 10.8 Hz, H-7a); 6.72 (d, 1H, *J* = 8.0 Hz, H-7′); 7.07−7.26 (m, 6H, H-4′, H-6′, and aryl); 7.72 (s, 1H, N*H*). ^{13}CNMR (100 MHz, $CDCl_3$) δ 21.2 (*C*H_3); 21.3 (*C*H_3); 32.5 (C-1), 42.9 (*C*H_2), 68.9 (C-7a), 70.2 (C-3), 110.7, 125.3, 126.1, 128.7, 129.5, 131.5, 133.6, 135.8, 138.0 (aryl), 156.5, 169.6, 176.1 (C═O). ESIMS *m*/*z* calcd for $C_{21}H_{19}N_3O_3S$, 393.11; found, 393.24.

(3*R*,7a*R*)-6-(4-Chlorobenzyl)-5′-methyl-1*H*-spiro[imidazo-[1,5-*c*]thiazole-3,3′-indoline]-2′,5,7(6*H*,7a*H*)-trione (10c). Yield 39%, mp 208−209 °C, $[\alpha]^{25}_D$ −14.5° (*c* 0.13, MeOH). ^{1}H NMR (400 MHz, $CDCl_3$) δ 2.29 (s, 3H, CH_3); 3.30 (dd, 1H, *J* = 5.6 and 11.6 Hz, Ha-1); 3.69 (t, 1H, Hb-1); 4.50 (d, 1H, *J* = 15.2 Hz, CH_2); 4.63 (d, 1H, CH_2); 4.99 (dd, 1H, *J* = 4.8 and 10.4 Hz, H-7a); 6.72 (d, 1H, *J* = 8.0 Hz, H-7′); 7.05 (d, 1H, H-6′); 7.20−7.26 (m, 5H, H-4′ and aryl); 8.54 (s, 1H, N*H*). ^{13}C NMR (100 MHz, $CDCl_3$) δ 21.2 (*C*H_3); 32.3 (C-1), 42.4 (*C*H_2), 68.9 (C-7a), 70.3 (C-3), 110.9, 125.3, 126.0, 129.1, 130.1, 131.6, 133.3, 133.9, 134.2, 138.4 (aryl), 156.3, 169.9, 176.1 (C═O). ESIMS *m*/*z* calcd for $C_{20}H_{16}ClN_3O_3S$, 413.06; found, 413.17.

(3*R*,7a*R*)-5′-Methyl-6-(3,4,5-trimethoxybenzyl)-1*H*-spiro-[imidazo[1,5-*c*]thiazole-3,3′-indoline]-2′,5,7(6*H*,7a*H*)-trione (10d). Yield 47%, mp 241−242 °C, $[\alpha]^{25}_D$ −13.9° (*c* 0.11, MeOH). ^{1}H NMR (400 MHz, $CDCl_3$) δ 2.31 (s, 3H, CH_3); 3.28 (dd, 1H, *J* = 5.6 and 11.6 Hz, Ha-1); 3.64 (t, 1H, Hb-1); 3.73 (s 3H, OCH_3,); 3.76 (s 6H, OCH_3,); 4.39 (d, 1H, *J* = 14.8 Hz, CH_2); 4.59 (d, 1H, CH_2); 4.94 (dd, 1H, *J* = 5.6 and 10.8 Hz, H-7a); 6.50 (s 2H, aryl); 6.45 (d, 1H, *J* = 8.0 Hz, H-7′); 6.99 (d, 1H, H-6′); 7.16 (s, 1H, H-4′); 8.04 (s, 1H, N*H*). ^{13}C NMR (100 MHz, $CDCl_3$) δ 21.2 (*C*H_3); 32.5 (C-1), 43.4 (*C*H_2), 56.4 (O*C*H_3); 68.9 (C-7a), 70.6 (C-3), 105.5, 110.9, 125.3, 126.0, 131.1, 131.6, 133.4, 137.9, 138.2, 153.6 (aryl), 156.4, 169.9, 175.8 (C═O). ESIMS *m*/*z* calcd for $C_{23}H_{23}N_3O_6S$, 469.13; found, 469.32.

(3*R*,7a*R*)-6-(4,4-Dimethylcyclohexyl)-5′-methyl-1*H*-spiro-[imidazo[1,5-*c*]thiazole-3,3′-indoline]-2′,5,7(6*H*,7a*H*)-trione (10e). Yield 54%, mp 183−184 °C, $[\alpha]^{25}_D$ −13.6° (*c* 0.12, MeOH). ^{1}H NMR (400 MHz, $CDCl_3$) δ 0.89 (s, 3H, CH_3); 0.93 (s, 3H, CH_3); 1.18−1.30 (m, 2H, CH_2); 1.41−1.48 (m, 4H, CH_2); 2.21−2.29 (m, 2H, CH_2); 2.31 (s, 3H, CH_3); 3.32 (dd, 1H, *J* = 5.2 and 11.2 Hz, Ha-1); 3.71 (t, 1H, Hb-1); 3.73−3.82 (m, 1H, C*H*); 4.91 (dd, 1H, *J* = 5.6 and 10.8 Hz, H-7a); 6.75 (d, 1H, *J* = 8.0 Hz, H-7′); 7.08 (d, 1H, H-6′); 7.24 (s, 1H, H-4′); 7.90 (s, 1H, N*H*). ^{13}C NMR (100 MHz, $CDCl_3$) δ 22.4 (*C*H_3); 24.1 (*C*H_2); 24.9 (*C*H_2); 25.0 (*C*H_3); 29.7 (*C*H_3), 32.5 (C-1), 38.6 (*C*H), 52.5 (*C*), 68.4 (C-7a), 70.8 (C-3), 109.2, 125.0, 125.3, 131.1, 143.6 (aryl), 156.6, 170.5, 174.6 (C═O). ESIMS *m*/*z* calcd for $C_{21}H_{25}N_3O_3S$, 399.16; found, 399.21.

(3*R*,7a*R*)-6-(Benzyl)-5′-bromo-1*H*-spiro[imidazo[1,5-*c*]thiazole-3,3′-indoline]-2′,5,7(6*H*,7a*H*)-trione (11a). Yield 40%, mp 209−210 °C, $[\alpha]^{25}_D$ −11.8° (*c* 0.1, MeOH). ^{1}H NMR (400 MHz, $CDCl_3$) δ 3.35 (dd, 1H, *J* = 5.3 and 11.3 Hz, Ha-1); 3.72 (t, 1H, Hb-1); 4.56 (d, 1H, *J* = 14.8 Hz, C*H*$_2$); 4.71 (d, 1H, C*H*$_2$); 5.00 (dd, 1H, *J* = 5.6 and 11.1 Hz, H-7a); 6.77 (d, 1H, *J* = 7.2 Hz, H-7′); 7.26−7.32 (m, 5H, aryl); 7.43 (d, 1H, H-6′); 7.54 (s, 1H, H-4′); 8.01 (s, 1H, N*H*). ^{13}C NMR (100 MHz, $CDCl_3$) δ 32.3 (C-1), 43.9 (*C*H$_2$), 69.1 (C-7a), 72.2 (C-3), 113.3, 123.4, 125.8, 128.3, 130.2, 131.5, 133.6, 136.2, 139.1 (aryl), 156.1, 169.8, 175.8 (C═O). ESIMS *m*/*z* calcd for $C_{19}H_{14}BrN_3O_3S$, 442.99; found, 443.16.

Data for (3*R*,7a*R*)-5′-Bromo-6-(4-methybenzyl)-1*H*-spiro-[imidazo[1,5-*c*]thiazole-3,3′-indoline]-2′,5,7(6*H*,7a*H*)-trione (11b). Yield 39%, mp 233−234 °C, $[\alpha]^{25}_D$ −10.3° (*c* 0.1, MeOH). ^{1}H NMR (400 MHz, $CDCl_3$) δ 2.29 (s, 3H, C*H*$_3$); 3.33 (dd, 1H, *J* = 5.3 and 11.0 Hz, Ha-1); 3.71 (t, 1H, Hb-1); 4.51 (d, 1H, *J* = 14.5 Hz, C*H*$_2$); 4.67 (d, 1H, C*H*$_2$); 4.97 (dd, 1H, *J* = 5.6 and 10.8 Hz, H-7a); 6.79 (d, 1H, *J* = 7.5 Hz, H-7′); 7.04−7.11 (m, 4H, aryl); 7.41 (d, 1H, H-6′); 7.51 (s, 1H, H-4′); 8.00 (s, 1H, N*H*). ^{13}C NMR (100 MHz, $CDCl_3$) δ 21.5 (*C*H$_3$), 32.4 (C-1), 43.0 (*C*H$_2$), 68.9 (C-7a), 71.9 (C-3), 115.2, 125.3, 128.1, 129.4, 129.9, 132.9, 133.7, 136.2, 139.0 (aryl), 156.2, 169.6, 176.2 (C═O). ESIMS *m*/*z* calcd for $C_{20}H_{16}BrN_3O_3S$, 457.01; found, 457.11.

(3*R*,7a*R*)-5′-Bromo-6-(4-chlorobenzyl)-1*H*-spiro[imidazo[1,5-*c*]-thiazole-3,3′-indoline]-2′,5,7(6*H*,7a*H*)-trione (11c). Yield 38%, mp 202−203 °C, $[\alpha]^{25}_D$ −11.9° (*c* 0.11, MeOH). ^{1}H NMR (400 MHz, $CDCl_3$) δ 3.30 (dd, 1H, *J* = 5.5 and 11.1 Hz, Ha-1); 3.69 (t, 1H, Hb-1); 4.50 (d, 1H, *J* = 15.2 Hz, C*H*$_2$); 4.63 (d, 1H, C*H*$_2$); 4.98 (dd, 1H, *J* = 4.8 and 10.4 Hz, H-7a); 6.75 (d, 1H, *J* = 7.1 Hz, H-7′); 7.20−7.26 (m, 4H, aryl); 7.43 (d, 1H, H-6′); 7.55 (s, 1H, H-4′); 8.11 (s, 1H, N*H*). ^{13}C NMR (100 MHz, $CDCl_3$) δ 32.3 (C-1), 42.4 (*C*H$_2$), 69.0 (C-7a), 72.0 (C-3), 115.2, 125.3, 126.0, 129.1, 130.1, 132.1, 133.9, 134.2, 140.7 (aryl), 156.4, 168.9, 176.0 (C═O). ESIMS *m*/*z* calcd for $C_{19}H_{13}BrClN_3O_3S$, 476.95; found, 476.89

(3*R*,7a*R*)-5′-Bromo-6-(3,4,5-trimethoxybenzyl)-1*H*-spiro-[imidazo[1,5-*c*]thiazole-3,3′-indoline]-2′,5,7(6*H*,7a*H*)-trione (11d). Yield 40%, mp 255−256 °C, $[\alpha]^{25}_D$ −12.3° (*c* 0.13, MeOH). ^{1}H NMR (400 MHz, $CDCl_3$) δ 3.38 (dd, 1H, *J*′ = 5.6 and 11.6 Hz, Ha-1); 3.72 (t, 1H, Hb-1); 3.79 (s 3H, OC*H*$_3$,); 3.82 (s, 6H, OC*H*$_3$,); 4.47 (d, 1H, *J* = 14.4 Hz, C*H*$_2$); 4.64 (d, 1H, C*H*$_2$); 5.02 (dd, 1H, *J* = 5.2 and 10.4 Hz, H-7a); 6.51 (s, 2H, aryl); 6.77 (d, 1H, *J* = 7.2 Hz, H-7′); 7.45 (d, 1H, H-6′); 7.56 (s, 1H, H-4′); 8.02 (s, 1H, N*H*). ^{13}C NMR (100 MHz, $CDCl_3$) δ 32.5 (C-1), 43.3 (*C*H$_2$), 56.2 (O*C*H$_3$); 69.1 (C-7a), 71.9 (C-3), 105.3, 115.9, 125.6, 131.1, 131.6, 133.4, 137.9, 139.1, 153.6 (aryl), 156.4, 169.9, 175.8 (C═O). ESIMS *m*/*z* calcd for $C_{22}H_{20}BrN_3O_6S$, 533.03; found, 533.21.

(3*R*,7a*R*)-5′-Bromo-6-(4,4-dimethylcyclohexyl)-1*H*-spiro-[imidazo[1,5-*c*]thiazole-3,3′-indoline]-2′,5,7(6*H*,7a*H*)-trione (11e). Yield 42%, mp 200−201 °C, $[\alpha]^{25}_D$ −13.1° (*c* 0.12, MeOH). ^{1}H NMR (400 MHz, $CDCl_3$) δ 0.88 (s, 3H, C*H*$_3$); 0.92 (s, 3H, C*H*$_3$); 1.18−1.26 (m, 2H, C*H*$_2$); 1.41−1.49 (m, 4H, C*H*$_2$); 2.23−2.33 (m, 2H, C*H*$_2$); 3.32 (dd, 1H, *J* = 5.3 and 11.0 Hz, Ha-1); 3.71 (t, 1H, Hb-1); 3.78−3.82 (m, 1H, C*H*); 4.93 (dd, 1H, *J* = 5.3 and 10.8 Hz, H-7a); 6.73 (d, 1H, *J* = 7.01 Hz, H-7′); 7.46 (d, 1H, H-6′); 7.56 (s, 1H, H-4′); 8.00 (s, 1H, N*H*). ^{13}C NMR (100 MHz, $CDCl_3$) δ 24.9 (*C*H$_2$), 25.2 (*C*H$_2$), 27.9 (*C*H$_3$), 29.3 (*C*H$_3$), 32.4 (C-1), 38.9 (*C*H), 52.7 (*C*), 69.0 (C-7a), 71.6 (C-3), 116.1, 125.3, 131.1, 133.9, 140.1 (aryl), 156.6, 170.5, 174.6 (C═O). ESIMS *m*/*z* calcd for $C_{20}H_{22}BrN_3O_3S$, 463.06; found, 463.19.

(3*R*,7a*R*)-6-Benzyl-1′-methyl-1*H*-spiro[imidazo[1,5-*c*]thiazole-3,3′-indoline]-2′,5,7(6*H*,7a*H*)-trione (12a). Yield 46%, mp 177−178 °C, $[\alpha]^{25}_D$ −16.2° (*c* 0.11, MeOH). ^{1}H NMR (400 MHz, $CDCl_3$) δ 3.27 (s, 3H, C*H*$_3$); 3.35 (dd, 1H, *J* = 5.2 and 11.2 Hz, Ha-1); 3.76 (t, 1H, Hb-1); 4.54 (d, 1H, *J* = 14.4 Hz, C*H*$_2$); 4.71 (d, 1H, C*H*$_2$); 4.98 (dd, 1H, *J* = 5.6 and 11.2 Hz, H-7a); 6.86 (d, 1H, *J* = 8.0 Hz, H-7′); 7.10 (t, 1H, H-6′); 7.26−7.38 (m, 6H, H-5′ and aryl); 7.41 (d, 1H, H-4′). ^{13}C NMR (100 MHz, $CDCl_3$) δ 26.8 (*C*H$_3$), 32.4 (C-1), 42.9 (*C*H$_2$), 68.7 (C-7a), 70.3 (C-3), 110.0, 123.6, 125.4, 128.7, 129.9, 131.3, 132.6, 138.1, 143.8 (aryl), 156.2, 169.8, 174.5 (C═O). ESIMS *m*/*z* calcd for $C_{20}H_{17}N_3O_3S$, 379.10; found, 379.19.

(3*R*,7a*R*)-1′-Methyl-6-(4-methylbenzyl)-1*H*-spiro[imidazo-[1,5-*c*]thiazole-3,3′-indoline]-2′,5,7(6*H*,7a*H*)-trione (12b). Yield 48%, mp 185−186 °C, $[\alpha]^{25}_D$ −15.3° (*c* 0.1, MeOH). ^{1}H NMR (400 MHz, $CDCl_3$) δ 2.29 (s, 3H, C*H*$_3$); 3.28 (s, 3H, C*H*$_3$); 3.33 (dd, 1H, *J* = 5.2 and 10.8 Hz, Ha-1); 3.74 (t, 1H, Hb-1); 4.48 (d, 1H, *J* = 14.4 Hz, C*H*$_2$); 4.67 (d, 1H, C*H*$_2$); 4.96 (dd, 1H, *J* = 5.6 and 11.2 Hz, H-7a); 6.85 (d, 1H, *J* = 7.6 Hz, H-7′); 7.09−7.26 (m, 5H, H-6′ and aryl); 7.33−7.41 (m, 2H, H-5′ and H-4′). ^{13}C NMR (100 MHz, $CDCl_3$) δ 21.8 (*C*H$_3$), 26.9 (*C*H$_3$), 32.5 (C-1), 42.8 (*C*H$_2$), 68.9 (C-7a), 70.2 (C-3), 109.2, 123.7, 125.1, 128.8, 129.6, 131.2, 132.5, 138.0, 143.6 (aryl), 156.2, 169.8, 174.5 (C═O). ESIMS *m*/*z* calcd for $C_{21}H_{19}N_3O_3S$, 393.11; found, 393.25.

(3*R*,7a*R*)-6-(4-Chlorobenzyl)-1′-methyl-1*H*-spiro[imidazo-[1,5-*c*]thiazole-3,3′-indoline]-2′,5,7(6*H*,7a*H*)-trione (12c). Yield 41%, mp 182−183 °C, $[\alpha]^{25}_D$ −17.1° (*c* 0.13, MeOH). ^{1}H NMR (400 MHz, $CDCl_3$) δ 3.30 (s, 3H, C*H*$_3$); 3.33 (dd, 1H, *J* = 5.2 and 10.8 Hz, Ha-1); 3.74 (t, 1H, Hb-1); 4.49 (d, 1H, *J* = 14.4 Hz, C*H*$_2$); 4.67 (d, 1H, C*H*$_2$); 4.96 (dd, 1H, *J* = 5.6 and 11.2 Hz, H-7a); 6.85 (d, 1H, *J* = 8.0 Hz, H-7′); 7.09−7.26 (m, 5H, H-6′ and aryl); 7.33−7.41 (m, 2H, H-5′ and H-4′); ^{13}C NMR (100 MHz, $CDCl_3$) δ 26.4 (*C*H$_3$); 32.7 (C-1), 42.8 (*C*H$_2$), 68.9 (C-7a), 70.4 (C-3), 110.9, 125.6, 126.2, 129.3, 130.4, 131.7, 133.5, 133.8, 134.1, 138.2 (aryl), 156.3, 169.9, 176.3 (C═O). ESIMS *m*/*z* calcd for $C_{20}H_{16}ClN_3O_3S$, 413.06; found, 413.12.

(3*R*,7a*R*)-1′-Methyl-6-(3,4,5-trimethoxybenzyl)-1*H*-spiro-[imidazo[1,5-*c*]thiazole-3,3′-indoline]-2′,5,7(6*H*,7a*H*)-trione (12d). Yield 53%, mp 197−198 °C, $[\alpha]^{25}_D$ −16.1° (*c* 0.1, MeOH). ^{1}H NMR (400 MHz, $CDCl_3$) δ 3.18 (s, 3H, C*H*$_3$,); 3.33 (dd, 1H, *J* = 5.6 and 11.6 Hz, Ha-1); 3.64 (t, 1H, Hb-1); 3.71 (s 3H, OC*H*$_3$,); 3.79 (s, 6H, OC*H*$_3$,); 4.48 (d, 1H, *J* = 14.4 Hz, C*H*$_2$); 4.62 (d, 1H, C*H*$_2$); 5.04 (dd, 1H, *J* = 5.2 and 10.4 Hz, H-7a); 6.48 (s 2H, benzyl); 6.81 (d, 1H, *J* = 7.2 Hz, H-7′); 7.12 (t, 1H, H-6′); 7.26 (t, 1H, H-5′); 7.35 (d, 1H, H4′). ^{13}C NMR (100 MHz, $CDCl_3$) δ, 26.2 (*C*H$_3$); 32.6 (C-1), 43.8 (*C*H$_2$), 56.7 (O*C*H$_3$); 68.9 (C-7a), 70.3 (C-3), 105.7, 110.6, 125.3, 126.1, 129.8, 133.4, 138.2, 153.6 (aryl), 156.5, 169.8, 175.6 (C═O). ESIMS *m*/*z* calcd for $C_{23}H_{23}N_3O_6S$, 469.13; found, 469.29.

(3*R*,7a*R*)-6-(4,4-Dimethylcyclohexyl)-1′-methyl-1*H*-spiro-[imidazo[1,5-*c*]thiazole-3,3′-indoline]-2′,5,7(6*H*,7a*H*)-trione (12e). Yield 56%, mp 174−175 °C, $[\alpha]^{25}_D$ −16.8° (*c* 0.1, MeOH). ^{1}H NMR (400 MHz, $CDCl_3$) δ 0.89 (s, 3H, C*H*$_3$); 0.94 (s, 3H, C*H*$_3$); 1.19−1.25 (m, 2H, C*H*$_2$); 1.41−1.50 (m, 4H, C*H*$_2$); 2.18−2.31 (m, 2H, C*H*$_2$); 3.26 (s, 3H, C*H*$_3$); 3.32 (dd, 1H, *J* = 5.2 and 10.8 Hz, Ha-1); 3.72 (t, 1H, Hb-1); 3.70−3.76 (m, 1H, C*H*); 4.90 (dd, 1H, *J* = 5.6 and 11.2 Hz, H-7a); 6.85 (d, 1H, *J* = 7.6 Hz, H-7′); 7.11 (t, 1H, H-6′); 7.34 (t, 1H, H-5′); 7.43 (d, 1H, H-4′). ^{13}C NMR (100 MHz, $CDCl_3$) δ 24.1 (*C*H$_2$); 24.9 (*C*H$_2$); 25.0 (*C*H$_3$); 26.9 (*C*H$_3$); 29.7 (*C*H$_3$); 32.5 (C-1), 38.6 (*C*H), 52.5 (*C*), 68.3 (C-7a), 70.7 (C-3), 109.2, 123.6, 125.3, 131.0, 143.5 (aryl), 156.5, 170.5, 174.6 (C═O). ESIMS *m*/*z* calcd for $C_{21}H_{25}N_3O_3S$, 399.16; found, 399.27.

General Procedure for the Synthesis of the (3*R*,7a*R*)-1′-Acyl-6-(benzylsubstituted)-1*H*-spiro[imidazo[1,5-*c*]thiazole-3,3′-indoline]-2′,5,7(6*H*,7a*H*)-trione Derivatives (13f−i/14f−i). 9c or **10d** (100 mg, 0.2 mmol) was dissolved in dichloromethane (10 mL), and the appropriate acyl chloride (benzoyl chloride, 4-methylbenzoyl chloride, 4-chlorobenzoyl chloride or butirroyl chloride, **f**−**i**) (0.22 mmol) and TEA (0.30 mmol) were added. The mixture was stirred at room temperature for 2 h. Then the organic solution was washed with 10% $NaHCO_3$ and water, dried over Na_2SO_4, and evaporated to dryness. Flash chromatography was performed on silica gel, using as eluent a mixture ethyl acetate/*n*-hexane, 1/3, to obtain the corresponding N-substituted derivatives as white solids.

(3*R*,7a*R*)-1′-Benzoyl-6-(4-chlorobenzyl)-1*H*-spiro[imidazo-[1,5-*c*]thiazole-3,3′-indoline]-2′,5,7(6*H*,7a*H*)-trione (13f). Yield 85%, mp 245−246 °C, $[\alpha]^{25}_D$ −9.3° (*c* 0.1, MeOH). ^{1}H NMR (400 MHz, $CDCl_3$) δ 3.36 (dd, 1H, *J* = 6.0 and 12.0 Hz, Ha-1); 3.60 (t, 1H, Hb-1); 4.45 (d, 1H, *J* = 14.4 Hz, C*H*$_2$); 4.63 (d, 1H, C*H*$_2$); 5.03 (dd, 1H, *J* = 5.6 and 10.8 Hz, H-7a); 7.29 (t, 1H, H-6′); 7.42−7.48 (m, 3H, H-5′ and aryl); 7.55 (d, 1H, H-4′); 7.61 (t, 1H, aryl); 7.77−7.80 (m, 2H, aryl); 7.83 (d, 1H, H-7′). ^{13}C NMR (100 MHz, $CDCl_3$) δ 32.8 (C-1), 42.4 (*C*H$_2$), 68.9 (C-7a), 71.5 (C-3), 115.2, 124.4, 125.5, 126.0, 128.7, 129.4, 130.1, 130.3, 131.7, 133.3, 137.6, 144.5 (aryl), 156.2, 167.8, 169.1, 174.3 (C═O). ESIMS *m*/*z* calcd for $C_{26}H_{18}ClN_3O_4S$, 503.07; found, 503.16.

(3*R*,7a*R*)-6-(4-Chlorobenzyl)-1′-(4-methylbenzoyl)-1*H*-spiro-[imidazo[1,5-*c*]thiazole-3,3′-indoline]-2′,5,7(6*H*,7a*H*)-trione (13g). Yield 87%, mp 261−262 °C, $[\alpha]^{25}_D$ −8.1° (*c* 0.1, MeOH). ^{1}H NMR (400 MHz, $CDCl_3$) δ 2.40 (s, 3H, C*H*$_3$); 3.35 (dd, 1H, *J* = 5.6 and 11.6 Hz, Ha-1); 3.62 (t, 1H, Hb-1); 4.46 (d, 1H, *J* = 14.8 Hz, C*H*$_2$); 4.61 (d, 1H, C*H*$_2$); 5.02 (dd, 1H, *J* = 5.2 and 10.8 Hz, H-7a); 7.24 (t, 1H, H-6′); 7.42 (t, 1H, H-5′); 7.56 (d, 1H, *J* = 8.0 Hz, H-4′); 7.78 (d, 2H, *J* = 8.0 Hz, aryl); 7.81 (d, 1H, H-7′); 7.59 (d, 2H, aryl); ^{13}C NMR (100 MHz, $CDCl_3$) δ 21.8 (*C*H$_3$), 32.7 (C-1), 42.5 (*C*H$_2$), 68.9 (C-7a), 70.7 (C-3), 115.7, 124.8, 125.2, 125.9, 128.9, 129.2, 129.9, 130.1, 130.2, 131.6, 133.7, 137.1, 144.6 (aryl), 156.6, 167.8, 169.5, 174.3 (C═O). ESIMS *m*/*z* calcd for $C_{27}H_{20}ClN_3O_4S$, 517.09; found, 517.19.

(3*R*,7a*R*)-1′-(4-Chlorobenzoyl)-6-(4-chlorobenzyl)-1*H*-spiro-[imidazo[1,5-*c*]thiazole-3,3′-indoline]-2′,5,7(6*H*,7a*H*)-trione (13h). Yield 90%, mp 258−259 °C, $[\alpha]^{25}_D$ −7.8° (*c* 0.12, MeOH). ^{1}H NMR (400 MHz, $CDCl_3$) δ 3.34 (dd, 1H, *J* = 5.6 and 11.6 Hz, Ha-1); 3.59 (t, 1H, Hb-1); 4.52 (d, 1H, *J* = 14.8 Hz, C*H*$_2$); 4.62 (d, 1H, C*H*$_2$); 5.02 (dd, 1H, *J* = 5.2 and 10.8 Hz, H-7a); 7.31 (t, 1H, H-6′); 7.43 (d, 2H, *J* = 8.0 Hz, aryl); 7.48 (t, 1H, H-5′); 7.53 (d, 1H, *J* = 8.0 Hz, H-4′); 7.78 (d, 2H, aryl); 7.87 (d, 1H, H-7′); ^{13}C NMR (100 MHz, $CDCl_3$) δ 32.5 (C-1), 43.6 (*C*H$_2$), 68.9 (C-7a), 70.9 (C-3), 115.8, 124.4, 125.3, 126.2, 128.8, 129.2, 130.0, 131.4, 131.7, 137.7, 137.9, 138.1, 139.0, 141.5 (aryl), 156.8, 167.6, 169.4, 174.1 (C═O). ESIMS *m*/*z* calcd for $C_{26}H_{17}Cl_2N_3O_4S$, 537.03; found, 537.12.

(3*R*,7a*R*)-1′-Butyryl-6-(4-chlorobenzyl)-1*H*-spiro[imidazo-[1,5-*c*]thiazole-3,3′-indoline]-2′,5,7(6*H*,7a*H*)-trione (13i). Yield 89%, mp 231−232 °C, $[\alpha]^{25}_D$ −7.3° (*c* 0.1, MeOH). ^{1}H NMR (400 MHz, $CDCl_3$) δ 1.04 (t, 3H, C*H*$_3$); 1.72−1.82 (m, 2H, C*H*$_2$); 2.96−3.08 (m, 2H, C*H*$_2$); 3.37 (dd, 1H, *J* = 5.6 and 11.6 Hz, Ha-1); 3.67 (t, 1H, Hb-1); 4.52 (d, 1H, *J* = 14.4 Hz, C*H*$_2$); 4.64 (d, 1H, C*H*$_2$); 5.01 (dd, 1H, *J* = 5.2 and 10.8 Hz, H-7a); 7.24 (t, 1H, H-6′); 7.41 (t, 1H, H-5′); 7.47 (d, 1H, *J* = 8.0 Hz, H-4′); 8.25 (d, 1H, H-7′); ^{13}C NMR (100 MHz, $CDCl_3$) δ 13.9 (*C*H$_3$), 17.9 (*C*H$_2$), 32.8 (C-1), 40.4 (*C*H$_2$), 42.6 (*C*H$_2$), 68.9 (C-7a), 71.3 (C-3), 117.5, 124.3, 124.9, 126.1, 129.2, 130.2, 131.7, 133.7, 134.4, 140.1 (aryl), 157.3, 169.5, 173.7, 175.2 (C═O). ESIMS *m*/*z* calcd for $C_{23}H_{20}ClN_3O_4S$, 469.09; found, 469.18.

(3*R*,7a*R*)-1′-Benzoyl-5′-methyl-6-(3,4,5-trimethoxybenzyl)-1*H*-spiro[imidazo[1,5-*c*]thiazole-3,3′-indoline]-2′,5,7(6*H*,7a*H*)-trione (14f). Yield 87%, mp 271−273 °C, $[\alpha]^{25}_D$ −11.8° (*c* 0.11, MeOH). ^{1}H NMR (400 MHz, $CDCl_3$) δ 2.39 (s, 3H, C*H*$_3$); 3.34 (dd, 1H, *J* = 6.0 and 12.0 Hz, Ha-1); 3.59 (t, 1H, Hb-1); 3.66 (s, 3H, OC*H*$_3$,); 3.78 (s, 6H, OC*H*$_3$,); 4.43 (d, 1H, *J* = 14.4 Hz, C*H*$_2$); 4.62 (d, 1H, C*H*$_2$); 5.02 (dd, 1H, *J* = 5.6 and 10.8 Hz, H-7a); 6.47 (s, 2H, aryl); 7.23−7.26 (m, 2H, H-6′ and H-7′); 7.36 (s, 1H, H-4′); 7.41−7.45 (m, 2H, aryl); 7.58 (t, 1H, aryl); 7.80−7.83 (m, 2H, aryl). ^{13}C NMR (100 MHz, $CDCl_3$) δ 21.5 (*C*H$_3$); 32.4 (C-1), 42.8 (*C*H$_2$), 56.9 (O*C*H$_3$), 68.9 (C-7a), 71.2 (C-3), 105.5, 115.9, 124.6, 125.8, 126.9, 128.7, 129.3, 130.2, 131.8, 131.3, 132.0, 133.6, 153.5 (aryl), 156.6, 167.2, 169.4, 174.1 (C═O). ESIMS *m*/*z* calcd for $C_{30}H_{27}N_3O_7S$, 573.16; found, 573.21.

(3*R*,7a*R*)-5′-Methyl-1′-(4-methylbenzoyl)-6-(3,4,5-trimethoxybenzyl)-1*H*-spiro[imidazo[1,5-*c*]thiazole-3,3′-indoline]-2′,5,7-(6*H*,7a*H*)-trione (14g). Yield 89%, mp 293−294 °C, $[\alpha]^{25}_D$ −12.7° (*c* 0.11, MeOH). ^{1}H NMR (400 MHz, $CDCl_3$) δ 2.38 (s, 3H, C*H*$_3$); 2.42 (s, 3H, C*H*$_3$); 3.33 (dd, 1H, *J* = 5.6 and 11.6 Hz, Ha-1); 3.60 (t, 1H, Hb-1); 3.67 (s 3H, OC*H*$_3$,); 3.76 (s, 6H, OC*H*$_3$,); 4.42 (d, 1H, *J* = 14.8 Hz, C*H*$_2$); 4.62 (d, 1H, C*H*$_2$); 5.01 (dd, 1H, *J* = 5.2 and 10.8 Hz, H-7a); 6.49 (s 2H, aryl); 7.23−7.26 (m, 3H, H-6′, H-7′ and aryl); 7.35 (s, 1H, H-4′); 7.71−7.77 (m, 3H, aryl). ^{13}C NMR (100 MHz, $CDCl_3$) δ: 21.2 (*C*H$_3$); 21.8 (*C*H$_3$), 32.6 (C-1), 42.7 (*C*H$_2$), 56.5 (O*C*H$_3$), 68.8 (C-7a), 70.9 (C-3), 105.4, 115.8, 124.7, 125.5, 128.9, 129.6, 130.4, 131.5, 131.6, 132.9, 133.6, 137.3, 154.0 (aryl), 156.8, 167.3, 169.1, 174.3 (C═O). ESIMS *m*/*z* calcd for $C_{31}H_{29}N_3O_7S$, 587.17; found, 587.29.

(3*R*,7a*R*)-1′-(4-Chlorobenzoyl)-5′-methyl-6-(3,4,5-trimethoxybenzyl)-1*H*-spiro[imidazo[1,5-*c*]thiazole-3,3′-indoline]-2′,5,7-(6*H*,7a*H*)-trione (14h). Yield 91%, mp 280−281 °C, $[\alpha]^{25}_D$ −13.5° (*c* 0.13, MeOH). ^{1}H NMR (400 MHz, $CDCl_3$) δ 2.39 (s, 3H, C*H*$_3$); 3.32 (dd, 1H, *J*′ = 5.6 and 11.6 Hz, Ha-1); 3.61 (t, 1H, Hb-1); 3.69 (s, 3H, OC*H*$_3$,); 3.77 (s, 6H, OC*H*$_3$,); 4.43 (d, 1H, *J* = 14.8 Hz, C*H*$_2$); 4.64 (d, 1H, C*H*$_2$); 5.03 (dd, 1H, *J* = 5.2 and 10.8 Hz, H-7a); 6.49 (s, 2H, aryl); 7.26 (d, 1H, *J* = 8.0 Hz, H-7′); 7.36 (s, 1H, H-4′); 7.41−7.44 (m, 2H, H-6′, and aryl); 7.72−7.83 (m, 3H, aryl). ^{13}C NMR (100 MHz, $CDCl_3$) δ 21.4 (*C*H$_3$); 32.9 (C-1), 43.5 (*C*H$_2$), 56.3 (O*C*H$_3$), 68.9 (C-7a), 71.3 (C-3), 105.1, 115.8, 124.4, 125.6, 128.8, 129.1, 130.8, 131.2, 131.8, 132.2, 136.3, 137.4, 137.9, 139.7, 153.6 (aryl), 156.7, 167.7, 169.5, 174.4 (C═O). ESIMS *m*/*z* calcd for $C_{30}H_{26}ClN_3O_7S$, 607.12; found, 607.22.

(3*R*,7a*R*)-1′-Butyryl-5′-methyl-6-(3,4,5-trimethoxybenzyl)-1*H*-spiro[imidazo[1,5-*c*]thiazole-3,3′-indoline]-2′,5,7(6*H*,7a*H*)-trione (14i). Yield 91%, mp 258−259 °C, $[\alpha]^{25}_D$ −14.2° (*c* 0.15, MeOH). ^{1}H NMR (400 MHz, $CDCl_3$) δ 1.00 (t, 3H, C*H*$_3$); 1.73−1.80 (m, 2H, C*H*$_2$); 2.32 (s, 3H, C*H*$_3$); 3.00 (t, 2H, C*H*$_2$); 3.37 (dd, 1H, *J* = 5.6 and 11.6 Hz, Ha-1); 3.65 (t, 1H, Hb-1); 3.81 (s, 3H, OC*H*$_3$); 3.85 (s, 6H, OC*H*$_3$,); 4.45 (d, 1H, *J* = 14.4 Hz, C*H*$_2$); 4.62 (d, 1H, C*H*$_2$); 5.03 (dd, 1H, *J* = 5.2 and 10.8 Hz, H-7a); 6.56 (s, 2H, aryl); 7.21 (d, 1H, *J* = 8.0 Hz, H-7′); 7.28 (s, 1H, H-4′); 8.12 (d, 1H, H-6′). ^{13}C NMR (100 MHz, $CDCl_3$) δ: 13.5 (*C*H$_3$), 17.6 (*C*H$_2$), 21.5 (*C*H$_3$), 32.7 (C-1), 40.6 (*C*H$_2$), 42.9 (*C*H$_2$), 56.6 (O*C*H$_3$), 68.9 (C-7a), 71.5 (C-3), 105.6, 117.2, 124.6, 125.8, 129.1, 130.4, 131.3, 137.7, 139.5, 152.1 (aryl), 157.1, 169.7, 173.2, 175.7 (C═O). ESIMS *m*/*z* calcd for $C_{27}H_{29}N_3O_7S$, 539.17; found, 539.28.

Biology. Dulbecco's modified Eagle's medium (DMEM), fetal bovine serum (FBS), trypsin−EDTA solution (1×), penicillin and streptomycin, phosphate-buffered saline (PBS) were from Cambrex Biosciences. 3-(4,5-Dimethylthiazol-2-yl)-2,5-diphenyltetrazolium bromide (MTT), propidium iodide (PI), Triton X-100, sodium citrate, formamide, mouse monoclonal anti-tubulin were purchased from Sigma (Milan, Italy). Rabbit polyclonal anti-caspase-3, mouse monoclonal anti-PARP-1, mouse monoclonal anti-actin, mouse monoclonal anti-p53, and horseradish peroxidase (HRP) conjugated anti-mouse and anti-rabbit secondary antibodies were purchased from Santa Cruz Biotechnology (DBA; Milan, Italy). Rabbit polyclonal anti-cyclin B1 primary antibody were from Cell Signaling Technology (Celbio; Milan, Italy). ECL reagent was obtained from Amersham Pharmacia Biotech, U.K.

Cell Culture. Human embryonic kidney HEK 293, human melanoma M14, human monocytic leukemia U937, human normal thyroid TAD-2, and human papillary thyroid carcinoma TPC1 cell lines cell lines were grown at 37 °C in Dulbecco's modified Eagle's medium containing 10 mM glucose (DMEM-HG) supplemented with 10% fetal calf serum and 100 units/mL each of penicillin and streptomycin and 2 mmol/L glutamine. In each experiment, cells were placed in fresh medium, cultured in the presence of synthesized compounds (from 0.1 to 25 mM), and followed for further analyses.

Cell Viability Assay. Cell viability for M14, HEK, U937, TPC1n, and TAD-2 cell lines was determined using the 3-[4,5-dimethylthiazol-2,5-diphenyl-2*H*-tetrazolium bromide (MTT)

colorimetric assay. The test is based on the ability of mitochondrial dehydrogenase to convert, in viable cells, the yellow MTT reagent (Sigma Chemical Co., St. Louis, MO) into a soluble blue formazan dye. Cells were seeded into 96-well plates to a density of 105 cells/100 μL well. After 24 h of growth to allow attachment to the wells, compounds were added at various concentrations (from 0.1 to 25 mM). After 24 or 48 h of growth and after removal of the culture medium, 100 μL/well of medium containing 1 mg/mL of MTT was added. Cell cultures were further incubated at 37 °C for 2 h in the dark. The solution was then gently aspirated from each well, and the formazan crystals within the cells were dissolved with 100 μL of DMSO. Optical densities were read at 550 nm using a Multiskan Spectrum Thermo Electron Corporation reader. Results were expressed as percentage relative to vehicle-treated control (0.5% DMSO was added to untreated cells). IC_{50} (concentration eliciting 50% inhibition) values were determined by linear and polynomial regression. Experiments were performed in triplicate.

Time-Lapse Microscopy. Logarithmically growing M14 cells were placed in 96-well tissue culture plates at 10^5 cells/mL. After 24 h cells were incubated with a concentration corresponding to the IC_{50} of the various synthesized compounds and observed under an inverted phase-contrast microscope (Leica CTR6500 microscope). Images were captured every hour for 72 h. Plates (96-well) were incubated under standard culture conditions and kept at 37 °C in a 5% CO_2 atmosphere for the observation period (up to 72 h).

Flow Cytometry. M14 cells ($2{,}5 \times 10^5$ cells/mL) in 12-well tissue culture plates were incubated for 24 h in the presence or absence (vehicle-treated cells) of **9c** and **10d**. Cells were then washed with PBS 1× and suspended by trypsinization. Cells were centrifuged at 2000 rpm for 5 min, then washed with PBS 1× and resuspended in fresh medium. Finally, cells were incubated in the dark with a staining solution containing 0.1% sodium citrate, 0.1% Triton X-100, and 50 mg/mL propidium iodide at 4 °C for 30 min. Samples were analyzed by Becton Dickinson FACScan flow cytometer. The cell cycle distribution, expressed as percentage of cells in the G0/G1, S, and G2/M phages, was calculated using ModFit LT 3.0 software. Apoptotic cells are expressed as percentage of hypodiploid nuclei.

Western Blotting Analysis. M14 cells were plated in flasks (1×10^6 cells) in normal culture conditions and incubated with or without **9c** and **10d**. At the indicated times, cells were lysed using an ice cold lysis buffer (50 mM Tris, 150 mM NaCl, 10 mM EDTA, 1% Triton) supplemented with a mixture of protease inhibitors containing antipain, bestatin, chymostatin, leupeptin, pepstatin, phosphoramidon, Pefabloc, EDTA, and aprotinin (Boehringer, Mannheim, Germany). Equivalent amounts of protein were loaded on 8−12% sodium dodecyl sulfate (SDS)−polyacrylamide gels and electrophoresed followed by blotting onto nitrocellulose membranes (Bio-Rad, Germany). After blotting with 5% (w/v) fat-free milk powder and 0.1% Tween 20 in TBS, the membrane was incubated overnight at 4 °C with specific antibodies at the concentrations indicated by the manufacter's protocol (Santa Cruz Biotechnology). The antibody was diluted in Tris-buffered saline/Tween 20 5% milk powder. Following incubation with horseradish peroxidase-conjugated secondary antibodies, bands were detected by enhanced chemiluminescence (ECL kit, Amersham, Germany). Each filter was then probed with mouse monoclonal anti-tubulin antibody. Level of expression of detected bands was quantified by NIH ImageJ 1.40 after normalization with α-tubulin.

Statistical Analysis. Data were analyzed using Prism 4.0 (GraphPad Software, Inc.). Results are expressed as the mean ± SEM. All statistical differences were evaluated by a two tailed Student's *t* test and one way ANOVA. *P* values less than 0.05 were considered statistically significant.

Protein Expression and Purification for NMR Study. The recombinant human MDM2 (residues 1−118) was overexpressed in *E. coli* BL21(DE3) RIL using the pET-46Ek/LIC vector (Novagen). Cells were grown at 37 °C and induced with 1 mM IPTG at an OD_{600} of 0.7. The protein was purified and renatured from inclusion bodies as described.[28] The refolded protein was applied on butyl Sepharose 4 Fast Flow (Amersham) and then purified on a Sephadex G-75. The recombinant human p53 protein (residues 1−312) was overexpressed at 37 °C in *E. coli* BL21 (DE3) RIL using a pET-46Ek/LIC vector (Novagen) modified with N-terminal His-tag. The protein was purified under denaturing conditions using a NiNTA (Qiagen) column, refolded, and further purified using a gel filtration on Sephadex G-75 as previously described.[28] Complexes were made by mixing p53 and MDM2 in a molar ratio of 1:2. The excess of MDM2 was then removed by gel filtration on Sephadex G-75.

NMR Study of p53−MDM2 Interaction. NMR spectra were acquired at 25 °C on a Varian Unity INOVA 700 MHz spectrometer equipped with a cryoprobe. Typically, NMR samples contained up to 0.1 mM protein in 50 mM KH_2PO_4, 50 mM Na_2HPO_4, 150 mM NaCl, pH 7.4, 5 mM DTT, 0.02% NaN_3. Water suppression was carried out by gradient echo.[30] NMR data were processed using the Bruker program BioSpin 3.0. For NMR ligand binding experiments, 600 μL of the protein sample containing 10% D_2O, at ∼0.1 mM, and a 10 mM stock solution of each compound in DMSO-d_6 were used in all experiments. The final molar ratio protein/inhibitor was 1:1.

Acknowledgment. The ESIMS and NMR spectral data were provided by Centro di Ricerca Interdipartimentale di Analisi Strumentale, Università degli Studi di Napoli "Federico II". The assistance of the staff is gratefully appreciated. A.P., I.G., and B.M. were supported by a grant from the University of Salerno, Italy. We thank Prof. Tad A. Holak who kindly provided the plasmidic DNA coding for the two p53 and MDM2 constructor. We thank Dr. M. Illario and Dr. A. R. Rusciano for cytotoxic assay on TPC1 and TAD-2 cell lines.

Supporting Information Available: Microanalytical data for all test compounds. This material is available free of charge via the Internet at http://pubs.acs.org.

References

(1) Vogelstein, B.; Lane, D.; Levine, A. J. Surfing the p53 Network. *Nature* **2000**, *408*, 307–310.
(2) Vousden, K. H.; Lu, X. Live or Let Die: The Cell's Response to p53. *Nat. Rev. Cancer* **2002**, *2*, 594–604.
(3) Levine, A. J. P53, The Cellular Gatekeeper for Growth and Division. *Cell* **1997**, *88*, 323–331.
(4) (a) Hainaut, P.; Hollstein, M. P53 and Human Cancer: The First Ten Thousand Mutations. *Adv. Cancer Res.* **2000**, *77*, 81–137. (b) Olivier, M.; Eeles, R.; Hollstein, M.; Khan, M. A.; Harris, C. C.; Hainaut, P. The IARC TP53 Database: New Online Mutation Analysis and Recommendations to Users. *Hum. Mutat.* **2002**, *19*, 607–614.
(5) (a) Freedman, D. A.; Wu, L.; Levine, A. J. Functions of the MDM2 Oncoprotein. *Cell. Mol. Life Sci.* **1999**, *55*, 96–107. (b) Momand, J.; Wu, H. H.; Dasgupta, G. MDM2 Master Regulator of the p53 Tumor Suppressor Protein. *Gene* **2000**, *242*, 15–29.
(6) (a) Haupt, Y.; Maya, R.; Kazaz, A.; Moshe, O. Mdm2 Promotes the Rapid Degradation of p53. *Nature* **1997**, *387*, 296–299. (b) Kubbutat, M. H. G.; Jones, S. N.; Vousden, K. H. Regulation of p53 Stability by Mdm2. *Nature* **1997**, *387*, 299–303.
(7) Juven-Gershon, T.; Oren, M. Mdm2: The Ups and Downs. *Mol. Med.* **1999**, *5*, 71–83.
(8) (a) Fakharzadeh, S. S.; Trusko, S. P.; George, D. L. Tumorigenic Potential Associated with Enhanced Expression of a Gene That Is Amplified in a Mouse Tumor Cell Line. *EMBO J.* **1991**, *10*, 1565–1569. (b) Oliner, J. D.; Kinzler, K. W.; Meltzer, P. S.; George, D. L.; Vogelstein, B. Amplification of a Gene Encoding a p53-Associated Protein in Human Sarcomas. *Nature* **1992**, *358*, 80–83.
(9) Bottger, A.; Bottger, V.; Sparks, A.; Liu, W. L.; Howard, S. F.; Lane, D. P. Design of a Synthetic Mdm2-Binding Mini Protein that Activates the p53 Response in Vivo. *Curr. Biol.* **1997**, *7*, 860–869.
(10) (a) Chen, L.; Lu, W.; Agrawal, S.; Zhou, W.; Zhang, R.; Chen, J. Ubiquitous Induction of p53 in Tumor Cells by Antisense

Inhibition of MDM2 Expression. *Mol. Med.* **1999**, *5*, 21–34. (b) Zhang, Z.; Li, M.; Wang, H.; Agrawal, S.; Zhang, R. Antisense Therapy Targeting MDM2 Oncogene in Prostate Cancer: Effects on Proliferation, Apoptosis, Multiple Gene Expression, and Chemotherapy. *Proc. Natl. Acad. Sci. U.S.A.* **2003**, *100*, 11636–11641. (c) Wang, H.; Nan, L.; Yu, D.; Agrawal, S.; Zhang, R. Antisense Anti-MDM2 Oligonucleotides as a Novel Therapeutic Approach to Human Breast Cancer: In Vitro and in Vivo Activities and Mechanisms. *Clin. Cancer Res.* **2001**, *7*, 3613–3624.

(11) (a) Wasylyk, C.; Salvi, R.; Argentini, M.; Dureuil, C.; Delumeau, I.; Abecassis, J.; Debussche, L.; Wasylyk, B. P53 Mediated Death of Cells Overexpressing MDM2 by an Inhibitor of MDM2 Interaction with p53. *Oncogene* **1999**, *18*, 1921–1934. (b) Chene, P.; Fuchs, J.; Carena, I.; Furet, P.; Garcia-Echeverria, C. Study of the Cytotoxic Effect of a Peptidic Inhibitor of the p53−Hdm2 Interaction in Tumor Cells. *FEBS Lett.* **2002**, *529*, 293–297.

(12) (a) Klein, C.; Vassilev, L. T. Targeting the p53−MDM2 Interaction to Treat Cancer. *Br. J. Cancer* **2004**, *91*, 1415. (b) Vassilev, L. T. p53 Activation by Small Molecules: Application in Oncology. *J. Med. Chem.* **2005**, *48*, 4491–4499.

(13) (a) Chen, J.; Marechal, V.; Levine, A. J. Mapping of the p53 and Mdm-2 Interaction Domains. *Mol. Cell. Biol.* **1993**, *13*, 4107–4114. (b) Kussie, P. H.; Gorina, S.; Marechal, V.; Elenbaas, B.; Moreau, J.; Levine, A. J.; Pavletich, N. P. Structure of the MDM2 Oncoprotein Bound to the p53 Tumor Suppressor Transactivation Domain. *Science* **1996**, *274*, 948–953.

(14) (a) Murray, J. K.; Gellman, S. H. Targeting Protein−Protein Interactions: Lessons from p53/MDM2. *Biopolymers* **2007**, *88*, 657–686. (b) Shangary, S.; Wang, S. Small-Molecule Inhibitors of the MDM2−p53 Protein−Protein Interaction to Reactivate p53 Function: A Novel Approach for Cancer Therapy. *Annu. Rev. Pharmacol. Toxicol.* **2009**, *49*, 223–241.

(15) Zhao, J.; Wang, M.; Chen, J.; Luo, A.; Wanga, X.; Wua, M.; Yinb, D.; Liua, Z. The Initial Evaluation of Non-Peptidic Small-Molecule HDM2 Inhibitors Based on p53−HDM2 Complex Structure. *Cancer Lett.* **2002**, *183*, 69–77.

(16) Galatin, P. S.; Abraham, D. J. A Nonpeptidic Sulfonamide Inhibits the p53−mdm2 Interaction and Activates p53-Dependent Transcription in Mdm2-Overexpressing Cells. *J. Med. Chem.* **2004**, *47*, 4163–4165.

(17) Grasberger, B. L.; Lu, T.; Schubert, C.; Parks, D. J.; Carver, T. E.; Koblish, H. K.; Cummings, M. D.; LaFrance, L. V.; Milkiewicz, K. L.; Calvo, R. R.; Maguire, D.; Lattanze, J.; Franks, C. F.; Zhao, S.; Ramachandren, K.; Bylebyl, G. R.; Zhang, M.; Manthey, C. L.; Petrella, E. C.; Pantoliano, M. W.; Deckman, I. C.; Spurlino, J. C.; Maroney, A. C.; Tomczuk, B. E.; Molloy, C. J.; Bone, R. F. Discovery and Cocrystal Structure of Benzodiazepinedione HDM2 Antagonists That Activate p53 in Cells. *J. Med. Chem.* **2005**, *48*, 909–912.

(18) Vassilev, L. T.; Vu, B. T.; Graves, B.; Carvajal, D.; Podlaski, F.; Filipovic, Z.; Kong, N.; Kammlott, U.; Lukacs, C.; Klein, C.; Fotouhi, N.; Liu, E. A. In Vivo Activation of the p53 Pathway by Small-Molecule Antagonists of MDM2. *Science* **2004**, *303*, 844–848.

(19) (a) Ding, K.; Lu, Y.; Nikolovska-Coleska, Z.; Qui, S.; Ding, Y.; Gao, W.; Stuckey, J.; Krajewski, K.; Roller, P. P.; Tomita, Y.; Parrish, D. A.; Deschamps, J. R.; Wang, S. Structure-Based Design of Potent Non-Peptide MDM2 Inhibitors. *J. Am. Chem. Soc.* **2005**, *127*, 10130–10131. (b) Yu, S.; Qin, D.; Shangary, S.; Chen, J.; Wang, G.; Ding, K.; McEachern, D.; Qiu, S.; Nikolovska-Coleska, Z.; Miller, R.; Kang, S.; Yang, D.; Wang, S. Potent and Orally Active Small-Molecule Inhibitors of the MDM2−p53 Interaction. *J. Med. Chem.* **2009**, *52*, 7970–7973.

(20) Issaeva, N.; Bozko, P.; Enge, M.; Protopopova, M.; Verhoef, L. G. G. C.; Masucci, M.; Pramanik, A.; Selivanova, G. Small Molecule RITA Binds to p53, Blocks p53−HDM-2 Interaction and Activates p53 Function in Tumors. *Nat. Med.* **2004**, *10*, 1321–1328.

(21) Galliford, C. V.; Scheidt, K. A. Pyrrolidinyl-Spirooxindole Natural Products as Inspirations for the Development of Potential Therapeutic Agents. *Angew. Chem., Int. Ed.* **2007**, *46*, 8748–8758.

(22) Bertamino, A.; Aquino, C.; Sala, M.; de Simone, N.; Mattia, C. A.; Erra, L.; Musella, S.; Iannelli, P.; Carotenuto, A.; Grieco, P.; Novellino, E.; Campiglia, P.; Gomez- Monterrey, I. Design and Synthesis of Spirotryprostatin-Inspired Diketopiperazine Systems from Prolyl Spirooxoindolethiazolidine Derivatives. *Bioorg. Med. Chem.* **2010**, *18*, 4328–4337.

(23) Dömling, A. Small Molecular Weight Protein−Protein Interaction Antagonists—An Insurmountable Challenge? *Curr. Opin. Chem. Biol.* **2008**, *12*, 281–291.

(24) Miskolczi, I.; Zekany, A.; Rantal, F.; Linden, A.; Kover, K.; Gyorgydeak, Z. Diastereo- and Regioisomeric Bicyclic Thiohydantoins from Chiral 1,3-Thiazolidine-2,4-Dicarboxylic Acids. *Helv. Chim. Acta* **1998**, *81*, 744–753.

(25) Kerr, J. F. R.; Wyllie, A. H.; Currie, A. R. Apoptosis: A Basic Biological Phenomenon with Wide-Ranging Implications in Tissue Kinetics. *Br. J. Cancer* **1972**, *26*, 239–257.

(26) Jaanicke, R. U.; Sprengart, M. L.; Wati, M. R.; Porter, A. G. Caspase-3 Is Required for DNA Fragmentation and Morphological Changes Associated with Apoptosis. *J. Biol. Chem.* **1998**, *273*, 9357–9360.

(27) Germain, M.; Affar, E. B.; D'Amours, D.; Dixit, V. M.; Salvesen, G. S.; Poirier, G. G. Cleavage of Automodified Poly(ADP-ribose) Polymerase During Apoptosis. *J. Biol. Chem.* **1999**, *274*, 28379–28384.

(28) (a) D'Silva, L.; Ozdowy, P.; Krajewski, M.; Rothweiler, U.; Singh, M.; Holak, T. A. Monitoring the Effects of Antagonists on Protein−Protein Interactions with NMR Spectroscopy. *J. Am. Chem. Soc.* **2005**, *127*, 13220–13226. (b) Krajewski, M.; Rothweiler, U.; D'Silva, L.; Sudipta Majumdar, S.; Klein, C.; Holak., T. A. An NMR-Based Antagonist Induced Dissociation Assay for Targeting the Ligand−Protein and Protein−Protein Interactions in Competition Binding Experiments. *J. Med. Chem.* **2007**, *50*, 4382–4387.

(29) Dawson, R.; Mueller, L.; Dehner, A.; Klein, C.; Kessler, H.; Buchner, J. The N-terminal Domain of p53 Is Natively Unfolded. *J. Mol. Biol.* **2003**, *332*, 1131–1141.

(30) Hwang, T. L.; Shaka, A. J. Water Suppression That Works. Excitation Sculpting Using Arbitrary Wave-Forms and Pulsed-Field Gradients. *J. Magn. Reson.* **1995**, *112*, 275–279.